ELSEVIER

Global and Planetary Change 20 (1999) 93–123

GLOBAL AND PLANETARY CHANGE

Global sea level rise and glacial isostatic adjustment

W.R. Peltier *

Department of Physics, University of Toronto, 60 St. George Street, Toronto, Ontario, Canada M5S 1A7

Received 1 March 1997; received in revised form 15 March 1998

Abstract

The fact that the ongoing global process of glacial isostatic adjustment (GIA) contributes significantly to present-day observed rates of secular sea level change that are recorded on tide gauges is now rather well established. There is a continuing discussion, however, of the magnitude of the globally averaged rate of relative sea level rise that is residual to this GIA related 'contamination'. Accurate estimation of this residual is clearly important to the understanding of ongoing global change in the earth system. In the analyses presented herein, following a review of the global theory of the GIA process that focuses on the issue of rotational feedback, I begin by revisiting the issue of estimating this residual on the basis of secular sea level change measurements derived from long time series of annually averaged tide gauge recordings. These observations, all from the US east coast, are then decontaminated by subtracting estimates of the GIA effect determined on the basis of analysis of ^{14}C dated relative sea level histories to infer a (climate related?) residual signal. Also discussed herein, from a global modelling perspective, is the issue of the extent to which a globally averaged rate of sea level rise based upon TOPEX/POSEIDON type altimetric data (or secular gravity field data from the future GRACE mission) is expected to be contaminated by the GIA process. This issue has not been addressed previously and our analyses show that this contamination of the satellite altimeter estimated rate of global sea level rise will also be significantly influenced, locally, by ongoing glacial isostatic adjustment. However, when this signal is averaged over the surface track of TOPEX/POSEIDON we find that the extent to which this instrument's measure of the globally averaged rate of sea level rise is contaminated by the GIA process is small. © 1999 Elsevier Science B.V. All rights reserved.

Keywords: Sea level rise; Glacial isostatic adjustment; Contamination

1. Introduction

The issue of the existence, or otherwise, of a globally averaged positive rate of sea level rise has come to be seen as important to the understanding of global climate change (e.g., see Chapter 7 of Houghton et al., 1996 for a recent review). Until rather recently (Peltier and Tushingham, 1989), it was not clearly understood that even rather long tide gauge recordings of secular sea level change are significantly contaminated by a strong signal that is a relatively slowly varying function of latitude and longitude and which exists as a consequence of the last deglaciation event of the current ice-age. Beginning at LGM (Last Glacial Maximum) approximately 21,000 years ago, sea level rose on average over the ocean basins by an amount near 120 m due to the collapse of the large continental ice sheets that

* E-mail: peltier@atmosp.physics.utoronto.ca

0921-8181/99/$ - see front matter © 1999 Elsevier Science B.V. All rights reserved.
PII: S0921-8181(98)00066-6

existed at that time (e.g., Peltier, 1994). Although this deglaciation event was essentially complete by 6000 years ago, sea level has continued to change, essentially everywhere on the earth's surface, due to this cause. This continuing variation of sea level exists as a consequence of the earth's delayed viscoelastic response to the redistribution of mass on its surface that accompanied deglaciation. In regions that were previously glaciated, such as Canada and Northwestern Europe, relative sea level continues to fall at a rate that is primarily determined by the ongoing postglacial rebound of the crust and which may exceed 1 cm yr^{-1} (in the southeast Hudson Bay region of Canada, this rate is near 1.1 cm yr^{-1}). Even at sites that are well removed from the centres of glaciation, however, the rates of sea level change that exist as a consequence of ongoing glacial isostatic adjustment (GIA) are nonnegligible. In these 'far field' regions, the impact of ongoing GIA is primarily to cause sea level to fall as a consequence of the redistribution of water over the ocean basins that accompanies the changing shape of the Earth, a redistribution that is required in order to ensure that the surface of the oceans (the geoid) remains a gravitational equipotential. A primary goal in the present paper will be to document the detailed global properties of the signal that is expected to exist due to this cause and to compare it to appropriate observations where possible. These analyses should be seen as both complementing and extending previous work on this problem recently described in Peltier and Tushingham (1989, 1991), Douglas (1991, 1995), Peltier (1996a,b) Peltier and Jiang (1996a, 1997), and Douglas (1997).

The plan of the paper is as follows. In Section 2, I will provide a brief summary of the global theory of glacial isostatic adjustment that my colleagues and students and I have continued to develop over the past two decades. The predicted map of the present-day rate of relative sea level change that is delivered by this theory will also be discussed along with the influence of rotational feedback upon this signature of the GIA process. In Section 3, I revisit the analysis of US east coast relative sea level data discussed in Peltier (1996a,b) and Peltier and Jiang (1997) in order to demonstrate that modern rates of secular sea level rise, in at least this geographical region, are significantly in excess of the rates associated with the ongoing global process of glacial isostatic adjustment. Section 4 presents a new global theoretical prediction of the absolute rate of sea level change with respect to the centre of mass of the planet. This is the signal that should be observed using a TOPEX/POSEIDON type altimeter on board an artificial earth satellite, if the only process operating in the earth system were the global process of GIA. The influence of rotational feedback on this signal is also considered. Conclusions are presented in Section 5.

2. The global theory of glacial isostatic adjustment and relative sea level change

Throughout the late Quaternary epoch of Earth history, planetary climate has been exceptionally sensitive to the small changes in effective solar insolation caused by the changing geometry of Earth's orbit around the Sun. Although such orbital insolation variations are small, reaching no more than a few percent in received insolation during the summer season (e.g., Berger, 1978) and effectively averaging to zero over the course of a single year, they appear to have been sufficient to cause the 'ice-ages' that have dominated climate system variability in the latter half of the Pleistocene period (Hays et al., 1976). For the past 900,000 years of this period, the northern hemisphere continents have experienced a series of glaciation and deglaciation events that have occurred with 'clock-like' regularity, each cycle having a characteristic duration of approximately 100,000 years. During each glaciation phase of the cycle, sea level has fallen on average by approximately 120 m as freshwater produced by evaporation from the oceans has been deposited as snow at high northern latitudes. On the long timescale of 90,000 years characteristic of the glaciation phase of the cycle, the snow is transformed into ice under its own weight, the ice sheets eventually reaching thicknesses of approximately 4 km prior to the onset of the deglaciation phase of the cycle. The primary geographical centres of the northern hemisphere ice sheets during the glaciation phase of each cycle were Northwestern Europe and Northern North America. In the southern hemisphere, significant deglaciation also occurred in West Antarctica and in Western

Patagonia. In both the Northwestern European and North American regions of the northern hemisphere, the nuclei of the ice sheets were marine, the former area having separate ice-domes centred on the Barents Sea and the Gulf of Bothnia and the latter having the main ice dome centred on present-day Hudson Bay. The specific spatial distribution of ice that existed during the time of maximum glaciation of the most recent ice age cycle, which occurred 21,000 years ago, is documented in Peltier (1994).

During the deglaciation event which culminated with the essentially complete demise of these northern hemisphere continental ice sheets (save for that which remains over Greenland), sea level rose by approximately 120 m on average as meltwater returned to the ocean basins. Even if the Earth were perfectly rigid this deglaciation event would not have resulted in a uniform rise of sea level with respect to the surface of the solid Earth. This is a consequence of the fact that the surface of the ocean, the 'geoid' of classical geodesy, is constrained to lie on a surface of constant gravitational potential. On a perfectly rigid Earth, the water added to the ocean basins by the melting ice sheets would have to be distributed over these basins in such a way as to ensure that the equilibrium ocean surface remained an equipotential. In fact, the rheology of the mantle of the Earth is visco-elastic, and this characteristic is in no context made more strikingly manifest than in connection with the relative sea level changes that are induced by the glaciation–deglaciation process.

Over the course of the past two decades, beginning with the paper by Peltier (1974), an increasingly detailed and accurate theory has been developed with which glacial-cycle induced sea level variations may be predicted. This theory is embodied in a so-called 'Sea Level Equation', the most primitive form of which was first elaborated by Farrell and Clark (1976) using the results of Peltier (1974) and Peltier and Andrews (1976). In its most fully developed form, this equation may be written as:

$$S(\theta,\lambda,t) = C(\theta,\lambda,t)\left[\int_{-\infty}^{t} \mathrm{d}t' \int\int_{\Omega} \mathrm{d}\Omega' \left\{ L(\theta',\lambda',t') \times G_{\phi}^{L}(\gamma, t-t') + \psi^{\mathrm{R}}(\theta',\lambda',t') \times G_{\phi}^{T}(\gamma, t-t') \right\} + \frac{\Delta\Phi(t)}{g} \right] \qquad (1)$$

In Eq. (1), $S(\theta,\lambda,t)$ is the level of the sea relative to the dynamically changing level of the local surface of the solid earth on which θ is latitude and λ is longitude. The function $C(\theta,\lambda,t)$ is the so-called Ocean Function (Munk and MacDonald, 1960), which is by definition equal to unity where there is ocean and zero where there is land. Inland seas, whose surfaces do not generally sit on the same equipotential surface as that which defines the surface of the global ocean, are also regions for which $C = 0$. Because the area of the surface that is ocean changes with the variation of the surface ice load as low lying areas become inundated by the sea when the ice sheets melt, and once ice covered and submerged regions rise out of the sea as a consequence of the postglacial rebound phenomenon, the function C is clearly time dependent and this time dependence must be determined in the process of solving Eq. (1) as fully described in Peltier (1994). The expression in square brackets on the right-hand-side of Eq. (1) has the form of the sum of two triple convolution integrals. The first of these space–time convolutions is a convolution of the surface mass load L with the difference between the surface mass load Green function for the gravitational potential perturbation ϕ (Peltier and Andrews, 1976), scaled by g, and the Green function for radial displacement. This term is strongly dominant in Eq. (1) and for many purposes the second convolution of the perturbation of the centrifugal potential induced by the changing rotational state of the planet with the tidal Green function for the gravitational potential perturbation ϕ (e.g., Dahlen, 1976) on the deforming solid surface, may be safely neglected as it describes a second-order effect. The term $\Delta\Phi(t)/g$ is required to ensure that the surface load L conserves mass. The necessity of the introduction of this term may be understood on the basis of the composite property of L, namely that it may be written, and in general is written, as:

$$L(\theta,\lambda,t) = \rho_{\mathrm{I}} I(\theta,\lambda,t) + \rho_{\mathrm{w}} S(\theta,\lambda,t) \qquad (2)$$

in which ρ_{I} and ρ_{w} are the densities of ice and water, respectively, and I and S are the thicknesses of ice and water, respectively. Because of Eq. (2) it is clear that Eq. (1) is an integral equation because the unknown relative sea level history S appears both

on the left-hand-side and under the convolution integral on the right-hand-side.

Two methods have been employed in the past to solve Eq. (1). The first of these and the most primitive is the 'pseudo'-finite clement method first described in Peltier et al. (1978) and employed as basis for detailed analysis by Clark et al. (1978) and Wu and Peltier (1983). This method has recently been replaced by a considerably more accurate 'pseudo'-spectral method discussed in detail in Mitrovica and Peltier (1991). Because the influence on sea level of the time dependence of the ocean function C and of the potential perturbation caused by the changing rotation are both second-order effects, it proves advantageous to solve Eq. (1) using an iterative technique first elaborated with respect to the determination of the time dependence of C in Peltier (1994). This iterative procedure will be briefly discussed here.

Assuming C to be time-independent and initially neglecting ψ^{R}, then, given a space–time deglaciation history $I(\theta,\lambda,t)$, we may solve Eq. (1) to determine $S(\theta,\lambda,t)$ using the pseudo-spectral method. Since Eq. (1) is a construct of first order perturbation theory, it describes S relative to an arbitrary 'datum'. We may exploit this ambiguity of datum to iteratively construct a solution to Eq. (1) that is 'topographically self-consistent' (Peltier, 1994) as follows. We simply define a time independent datum $T'(\theta,\lambda)$ by requiring that

$$S(\theta,\lambda,t_{\mathrm{p}}) + T'(\theta,\lambda) = T_{\mathrm{p}}(\theta,\lambda) \tag{3}$$

in which $T_{\mathrm{p}}(\theta,\lambda)$ is the topography with respect to sea level of the present-day Earth, defined, say, by the ETOPO5 data set. The time t_{p} is the present time. Given $T'(\theta,\lambda)$ defined in this way, we may infer the topography with respect to sea level at any time in the past by computing:

$$T(\theta,\lambda,t) = S(\theta,\lambda,t) + \left[T_{\mathrm{p}}(\theta,\lambda) - S(\theta,\lambda,t_{\mathrm{p}})\right] \tag{4}$$

The true paleotopography, including the contribution from the ice sheets of thickness $I(\theta,\lambda,t)$, is then:

$$\mathrm{PT}(\theta,\lambda,t) = T(\theta,\lambda,t) + I(\theta,\lambda,t) \tag{5}$$

At any point in space and at any instant of time for which $\mathrm{PT} < 0$ we may assume that we have ocean (the only exception to this general rule concerns a number of low lying inland seas such as the Caspean Sea). If, with this caveat in mind, we define a first 'guess' for the time dependent ocean function as

$$\begin{aligned} C^1(\theta,\lambda,t) &= 1 \quad \text{for } \mathrm{PT} < 0 \\ C^1(\theta,\lambda,t) &= 0 \quad \text{for } \mathrm{PT} > 0 \end{aligned} \tag{6}$$

we may then solve Eq. (1) once more to determine a new field $T''(\theta,\lambda)$ and thus a new approximation to the time dependent ocean function $C^2(\theta,\lambda,t)$. In practise it is found that this procedure converges in just a few iterations. Convergence is rapid because the impact of the time dependence of the ocean function on sea level is, indeed, a second-order effect.

A further second-order effect can also be accommodated in the same iterative fashion, namely that associated with the contribution to the effective gravitational potential due to the change in the planet's rotational state caused by the glaciation–deglaciation process. Although a considerable amount of work has been devoted to understanding the rotational response of the planet to the ice-age related variations in surface mass load (Peltier, 1982; Wu and Peltier, 1984; Peltier and Jiang, 1996a; Peltier, 1997), there has been little work done on the problem of the additional variations of sea level that must be induced by the related variations of the centrifugal potential. This effect is in fact very simple to incorporate into Eq. (2) in the context of the iterative inversion scheme previously described by Peltier (1994). Knowing $S(\theta,\lambda,t)$ from the inversion of Eq. (1), along with $C(\theta,\lambda,t)$ determined as described above, then together with the input deglaciation history $I(\theta,\lambda,t)$ we have a complete history of the variation of surface mass load. Using the detailed theory described in Peltier (1982), Wu and Peltier (1984) and Peltier and Jiang (1996a), as slightly corrected in Peltier (1997), we may then compute the perturbations ω_i to the initial angular velocity vector $\Omega_0 \hat{x}_3$ of the visco-elastic planet on the basis of the assumption that $\omega_i/\Omega_0 \ll 1$ for all i ($i = 1, 3$ with $i = 3$ defining the direction of the angular velocity

vector in the unperturbed state). It is then a simple matter to compute the change in the centrifugal potential caused by the changing rotational state. This centrifugal potential, Ψ_t say, may be written in the form (e.g., Munk and MacDonald, 1960):

$$\Psi_t = \frac{1}{3}\omega_t^2 r^2 + \chi_t \tag{7}$$

in which:

$$\chi_t = \frac{1}{6}\left[\omega_1^2\left(x_2^2 + x_3^2 - 2x_1^2\right) + \ldots - 6\omega_1\omega_2 x_1 x_2\right] \tag{8}$$

is a spherical harmonic of degree 2 and the dots represent additional terms obtained by cyclic permutation of the indices. Recognizing that Eq. (7) is the total centrifugal potential we may determine the perturbation to the centrifugal potential caused by the time dependent rotational state induced by glaciation and deglaciation by evaluating $\psi' = \psi_t - \psi_0$ where ψ_0 at the initial centrifugal potential at the surface of the Earth where $r = a$. If we expand $\omega_t = (\omega_1,\ \omega_2,\ \omega_3)$ in the form:

$$\omega_1 = \omega_1' \tag{9a}$$

$$\omega_2 = \omega_2' \tag{9b}$$

$$\omega_3 = \omega_3' + \Omega_0 \tag{9c}$$

substitute into $\psi = \psi_t - \psi_0$, drop the primes and neglect second-order terms in the perturbations, we then obtain:

$$\psi = \psi_{00} Y_{00}(\theta,\lambda) + \sum_{m=-1}^{+1} \psi_{2m} Y_{2m}(\theta,\lambda) \tag{10}$$

where:

$$\psi_{00} = \frac{2}{3}\omega_3 \Omega_0 a^2 \tag{11a}$$

$$\psi_{20} = -\frac{1}{3}\omega_3 \Omega_0 a^2 \sqrt{4/5} \tag{11b}$$

$$\psi_{21} = (\omega_1 - i\omega_2)\left(\Omega_0 a^2/2\right)\sqrt{2/15} \tag{11c}$$

$$\psi_{2-1} = (\omega_1 + i\omega_2)\left(\Omega_0 a^2/2\right)\sqrt{2/15} \tag{11d}$$

Although one could easily obtain the spherical harmonic expansion of $\psi_t - \psi_0$ without dropping the second-order terms in the ω_i as has been done in deriving Eqs. (11a), (11b), (11c) and (11d), since the theory of Peltier (1982) and Wu and Peltier (1984) which is used to evaluate the $\omega_i(t)$ is a perturbation theory that is accurate only to first order in the ω_i, and since $\omega_i/\Omega_0 \ll 1$, it would appear to be inappropriate to retain nonlinear term in Eqs. (7) and (8). Careful inspection of Eqs. (10), (11a), (11b), (11c) and (11d), which is based upon the following normalization of the spherical harmonics:

$$\int\int Y_{\ell m} Y_{\ell' m'}\, \mathrm{d}\Omega = 4\pi \delta_{\ell'\ell}\delta_{m'm} \tag{12}$$

will demonstrate that this expression is essentially identical to that previously derived by Dahlen (1976) (see his eqs. 116 and 117) in his perfectly elastic analysis of the so-called 'pole-tide' produced in consequence of Earth's varying rotation. Milne and Mitrovica (1996) have described an initial attempt to incorporate the influence of the changing rotation on postglacial sea level histories and have also found that it is indeed a second-order effect. The precise global form of this effect will be much more fully discussed herein.

To complete the definitions of all terms appearing in the sea level Eq. (1), we require the Green functions G_ϕ^L and G_ϕ^T for the surface-load (L) and rotational (T for 'tidal') respective contributions to the net forcing. These Green functions may be evaluated using the theoretical methods developed in Peltier (1974, 1976, 1985) and they take the form:

$$G_\phi^L(\theta,\lambda,t) = \frac{a}{me}\sum_{\ell=0}^{\infty}\left(1 + k_\ell^L(t) - h_\ell^L(t)\right)P_\ell(\cos\theta) \tag{13a}$$

$$G_\phi^T(\theta,\lambda,t) = \frac{1}{g}\sum_{\ell=0}^{\infty}\left(1 + k_\ell^T(t) - h_\ell^T(t)\right)P_\ell(\cos\theta) \tag{13b}$$

in which $(k_\ell^L,\ h_\ell^L)$ and $(k_\ell^T,\ h_\ell^T)$ are visco-elastic surface load and tidal Love numbers of degree ℓ, respectively. The time dependence of these impulse response Love numbers depends upon the (assumed radial) visco-elastic structure of the planet. Assuming the rheology to be linearly visco-elastic and Maxwellian, then it is shown in these references that the $k_\ell^{L,T}$ and $h_\ell^{L,T}$ Love numbers may be represented in terms of a normal mode decomposition by a finite sum of purely exponential modes of relaxation (when the otherwise infinite sequence of transition modes (Peltier, 1976) is truncated by neglecting those whose contribution to the net viscous relaxation is less than some small prescribed cut-off). If we assume that the elastic part of the radial visco-elastic structure is fixed by seismology, say by the PREM model of Dziewonski and Anderson (1981), then the model for relative sea level history embodied in Eq. (1) is completely specified once we fix the radial profile of viscosity in the planetary mantle, $\nu(r)$ say, and the deglaciation history $I(\theta,\lambda,t)$. In order to illustrate the nature of the solutions delivered by Eq. (1), I will describe two solutions that differ from one another only in the radial viscosity profile for which they have been computed, the deglaciation history $I(\theta,\lambda,t)$ in each case being fixed to the ICE-4G model of Peltier (1994, 1996b). For one of these viscosity models, namely that preferred by the totality of the glacial isostatic adjustment observations, I will also describe the impact of rotational feedback on relative sea level history.

Fig. 1 shows a sequence of radial viscosity models that will be of interest to us in the context of the present paper. In plate (a) I have contrasted a simple two layer model called VM1 (dashed line) with a more complicated model called VM2, two versions of which are shown as bold and thin solid lines, respectively. The dashed line and the bold solid line are identical to the viscosity models described in Peltier (1996b) where they were referred to as M1 and M2, respectively. As discussed therein, model VM2 (M2) was derived from VM1 (M1) through a formal Bayesian inversion procedure using a large subset of glacial isostatic adjustment observations as in Peltier and Jiang (1996b). In Fig. 1, I have superimposed a new version of VM2 obtained by applying a minor variant of the inversion procedure. In this modified procedure I have simply substituted for the set of site specific relaxation time data deduced from the compilation of Tushingham and Peltier (1992), a revised set of relaxation time data for the same sites. These revised data were determined by Monte Carlo fit to the actual age-height pairs that define the emergence curve from these previously ice-covered locations rather than to the sampled envelope form of these data that was tabulated in Tushingham and Peltier (1992). Inspection of Fig. 1 shows that the viscosity model inferred on the basis of the formal inversion procedure is essentially insensitive to this variant on the inversion. The additional viscosity models displayed in plate (b) of Fig. 1 will be discussed further below.

Since the primary analyses for results which will be presented in this paper are to be those for the VM2 viscosity model, it will be useful to provide some evidence to the effect that this model does satisfactorily reconcile the primary observational constraints. To this end, I show on Fig. 2 a sequence

Fig. 1. Models of mantle viscosity inferred on the basis of the formal procedure described in Peltier (1996b). The data sets employed in the formal Bayesian inversions consist of (1) the relaxation spectrum for Fennoscandian rebound originally inferred by McConnell (1968), (2) a set of 25 site specific relaxation times for postglacial rebound inferred on the basis of Monte Carlo fits of an exponential model to individual ^{14}C dated relative sea level curves and (3) International Latitude Service data derived estimates of the present-day nontidal component of the acceleration of axial rotation (or equivalent $\dot{J}_2$) and the present-day rate and direction of true wander of the north pole of rotation. In (a), the dashed line is model VM1, whereas the heavy and light solid lines are the alternate versions of VM2 that the formal inversion procedure delivers when the 'sampled envelope' representation of individual relative sea level curves of Tushingham and Peltier (1992) is replaced by the 'raw' data themselves prior to application of the Monte Carlo procedure to deduce the site specific relaxation time. In (b) is shown the sequence of modifications to VM2 that the inversion procedure delivers when the ILS observation of $\dot{J}_2$ is modified to account for the contribution to it that would obtain if the observed global rate of sea level rise near 2 mm yr^{-1} were to be significantly associated with the melting of land ice from either Greenland or Antarctica at a rate from 0.5 to 1.5 mm yr^{-1}. Clearly, to the extent that this explanation of the ongoing global rise of sea level is correct, the rotational data then *require* significant elevation of the viscosity of the deepest mantle. The upper bound on lower mantle viscosity delivered by this analyses is near 10^{22} Pa s.

of intercomparisons between specific relative sea level data sets from sites near the centre of Laurentian rebound (Richmond Gulf, James Bay, the southeastern Hudson Bay Region as a whole) and the centre of Fennoscandia rebound (the Angerman River location). The 'data' shown in Fig. 2a are those taken from Hillaire-Marcel (1980), the circled crosses being uncalibrated ^{14}C measurements and the crosses representing beaches in Richmond Gulf for which age was estimated on the basis of the assumption that the process of beach formation was periodic with a period of 45 years. These points cannot

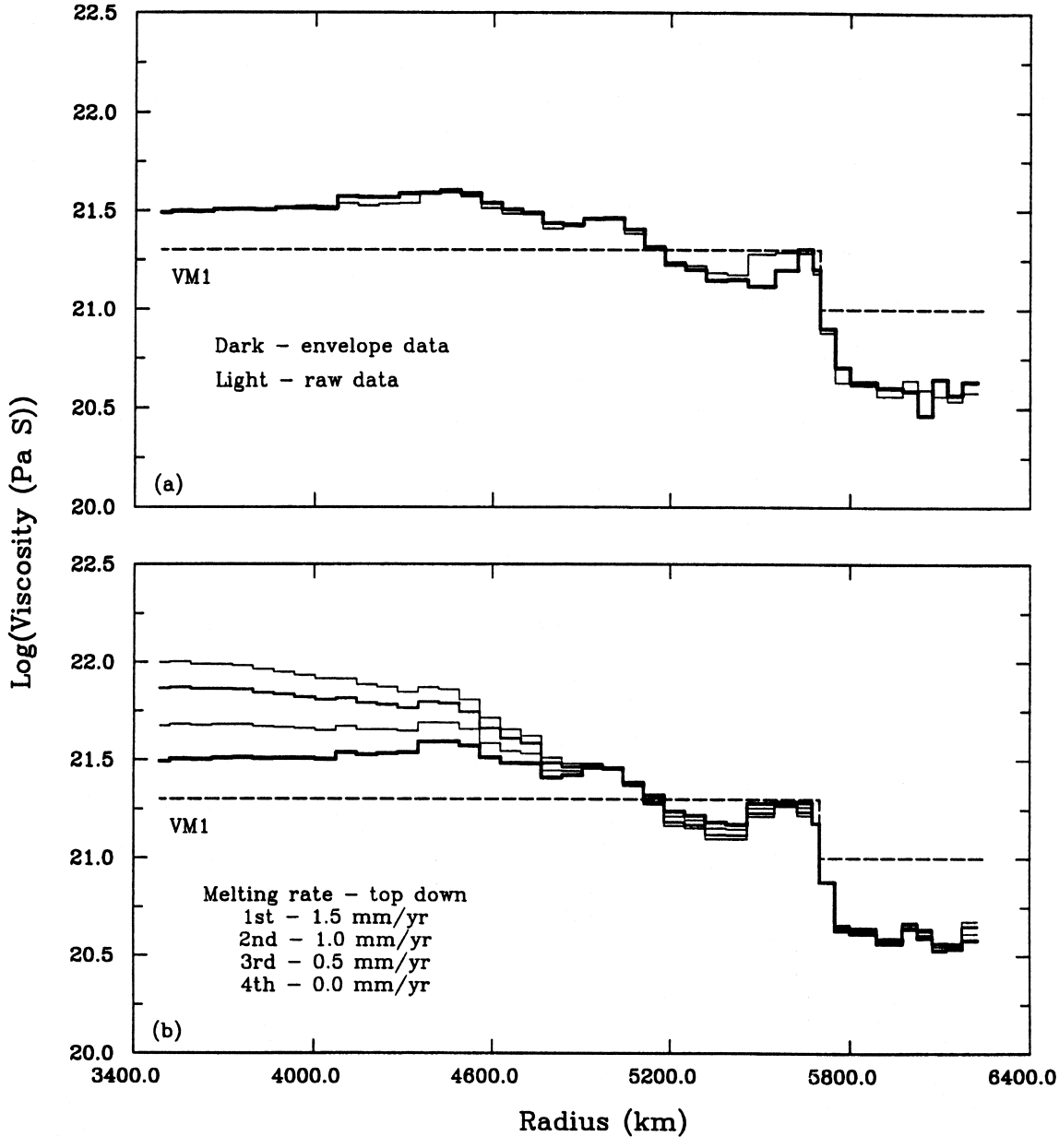

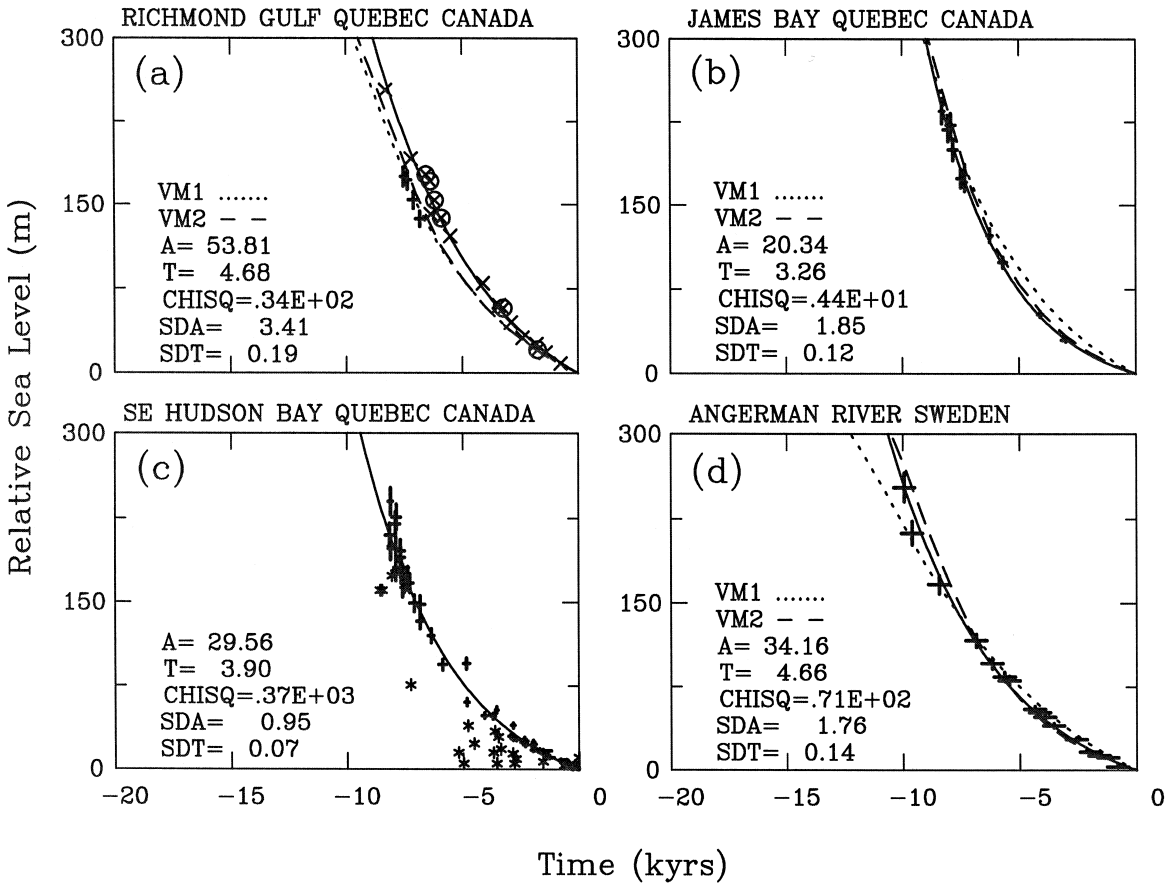

Fig. 2. (a) Relative sea level information from Richmond Gulf Quebec. ^{14}C data on the sidereal timescale of Hillaire-Marcel (1980) are shown as circled crosses and on the modern sidereal timescale of Stuiver and Reimer (1993) as plus signs. Crosses are not based upon the dating of actual sea level indicators but rather upon the assignment of ages to specific beach horizons based upon the assumption of a 45-year periodicity in the beach forming process. The solid curve is the exponential fit obtained to the original 'data set' of Hillaire-Marcel (1980) based upon a Monte Carlo inversion. The dotted and dashed curves are the theoretical predictions of rsl history at this site based upon the ICE-4G (VM1) and ICE-4G (MV2) models of Peltier (1994, 1996a,b). (b) Same as in (a) except for the James Bay site for which data are tabulated in Hardy (1976). On this figure are shown only the data selected by Hardy as providing the best constraints on relative sea level. (c) Same as (a) except that all of the data from the newly constructed data base for southeast Hudson Bay (Peltier, 1998) are plotted together. The data plotted as asterisks are those that have been culled for the purpose of determining the best-fitting exponential. (d) Same as (a) except for the Angerman River site in central Sweden.

therefore be construed to provide primary control. The dotted and dashed lines on the figure respectively represent the predicted histories of relative sea level based upon ICE-4G (VM1) and ICE-4G (VM2). When the small number of ^{14}C dates available to Hillaire–Marcel were properly calibrated to sidereal age, as they were in Walcott (1980), then these properly calibrated data fit extremely well to the predictions of both models. Also shown on Fig. 2a, and represented by the solid line, is a best fit exponential function of the form $\mathrm{rsl}(t) = A[e^{t/\tau} - 1]$ with A an amplitude in meters and τ a relaxation time in kiloyears. The parameters of this model determined by application of a Monte Carlo procedure to fit the data are also shown on the figure along with their (formal) standard deviations and the chi-squared

misfit of the exponential model to the data. Application of this procedure delivers $[A,\tau] = [53.81$ m, 4.68 kyr].

In Fig. 2b, an identical analysis is applied to the ^{14}C database of Hardy (1976) for the eastern James Bay region which is just to the south of Richmond Gulf and equivalently close to the centre of crustal rebound. With the ^{14}C data calibrated to give age in sidereal years by using the modern Calib. 3.0 programme of Stuiver and Reimer (1993) it will be clear that the fit of the VM2 model to the observations at James Bay is excellent whereas that of the VM1 model is slightly less satisfactory. Here, application of the Monte Carlo procedure to determine the parameters of the best fitting exponential model delivers $[A,\tau] = [20.34$ m, 3.26 kyr]. When the same analysis procedure is applied to the entire existing ^{14}C data base from southeastern Hudson Bay (see Peltier, 1998, for further discussion) then we obtain the result $[A,\tau] = [29.56$ m, 3.90 kyr]. Given the quality and quantity of data on which this estimate is based, I believe it to be the best available estimate of the relaxation time that has governed the postglacial rebound of the crust near the centre of uplift. It is furthermore highly significant that this estimate is intermediate between the predictions of the VM2 model for the Richmond Gulf ($[A,\tau] = [37.55$ m, 4.23 kyr]) and for James Bay ($[A,\tau] = [22.65$ m, 3.33 kyr]).

On Fig. 2d, I show the results obtained on the basis of a similar analysis of the data from the Angerman River in central Sweden which is close to the centre of the uplift forced by the disintegration of the Fennoscandian ice-sheet. Application of the Monte Carlo procedure to this data set delivers $[A,\tau] = [34.16$ m, 4.66 kyr]. Furthermore, it will be clear by inspection of the intercomparison between the VM1 and VM2 predictions and the Angerman River observations that the VM2 viscosity model is strongly preferred in this location as the relaxation time predicted by VM1 is far too long (see also Peltier, 1996b).

On Fig. 3 of this paper, I show in parts (a) and (b), respectively, a series of viscosity models recently analysed by Simons and Hager (1997) along with the version of the VM2 model discussed originally in Peltier (1976) which has been employed as basis for the preceding discussion. These viscosity models are respectively those of Lambeck et al. (1990) (LJN), Forte and Mitrovica (1996) (FM), Hager and Clayton (1989) (HC) and Simons and Hager (1997) (SH). In part (b) of this Fig. 1 show the predicted relaxation times at Richmond Gulf and Angerman River for each of these models along with the relaxation times inferred on the basis of the Monte Carlo inversions. Although all of the viscosity models adequately fit the observed relaxation time at Angerman River, only one of these models (VM2) also fits the observed relaxation time at the centre of Laurentian uplift. It is for this reason that I employ this model as the primary basis of discussion in all that follows.

In Fig. 4, I show global maps of the predicted present-day rate of relative sea level rise for both the VM1 and VM2 models of the radial viscosity profile as well as the difference between them. Inspection of this figure demonstrates that the greatest difference between the predictions of these two models exists along the east coast of the continental United States. In Section 3 of this paper we will consider the observed record of relative sea level history from this region in order to revisit the issue of the improvement of the fit of the global model of GIA to these data which is obtained when VM1 is replaced by VM2 (Peltier, 1996b).

Fig. 5 presents predictions of the present-day rate of relative sea level rise for the ICE-4G (VM2) model both including (+ ROT) and excluding (VM2) the influence of rotational feedback as well as the difference between these two calculations. The rotational response was first computed using the theory of Peltier (1982) and Wu and Peltier (1984) then inserted into Eq. (1) using Eq. (10) to evaluate the change of the centrifugal potential. With this perturbation added to the original kernel of Eq. (1), the sea level equation was solved once more to obtain the final result shown on Fig. 5. Details of the rotational response calculation using the ICE-4G model will be found in Peltier and Jiang (1996b) and Peltier (1997). It is useful to note that there is now agreement in the literature concerning the accuracy of the Peltier (1982) and Wu and Peltier (1984) theory of the rotational response to the ice-age cycle (see Vermeersen and Sabadini, 1996). It is also useful to note that both Milne and Mitrovica (1996) and Vermeersen and Sabadini (1996) have managed to re-

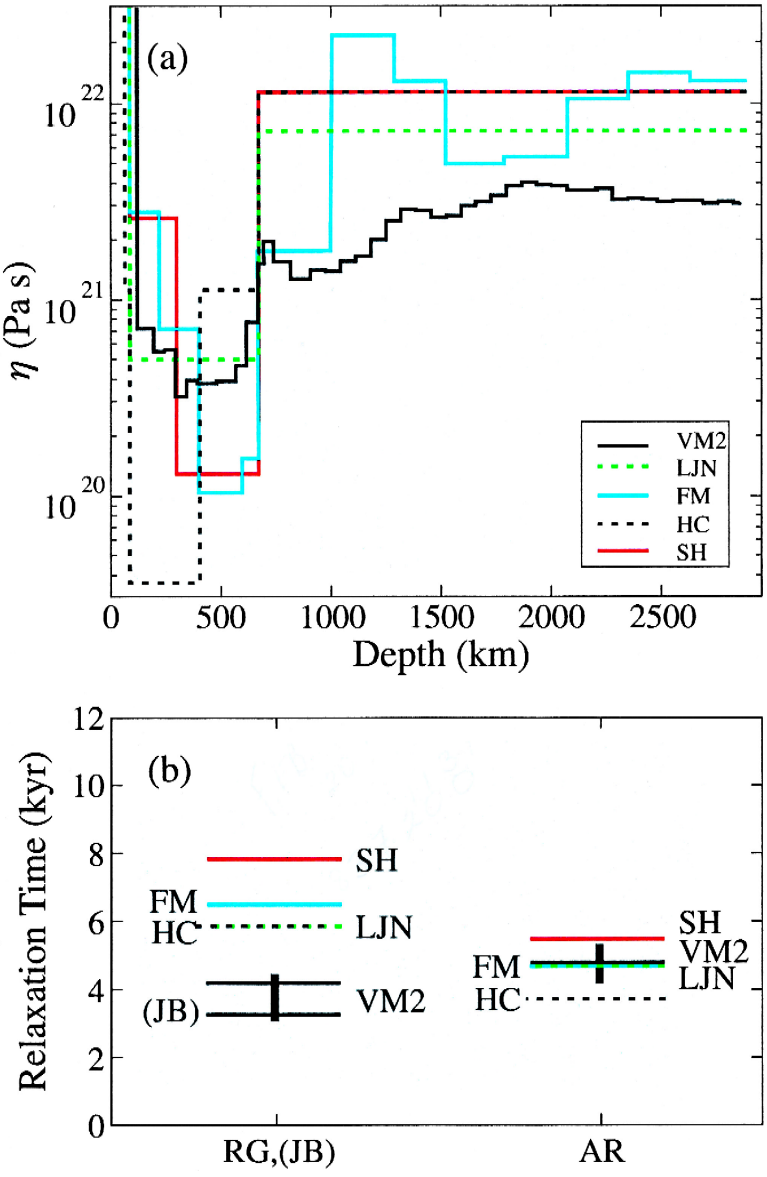

Fig. 3. (a) Viscosity models considered in Simons and Hager (1997) as well as the VM2 model for which analyses are presented herein. Viscosity models HC, LJN, FM and SH are described respectively by Hager and Clayton (1989), Lambeck et al. (1990), Forte and Mitrovica (1996) and Simons and Hager (1997). (b) Theoretical predictions of the relaxation time for postglacial rebound at Richmond Gulf and James Bay (Canada) and for Angerman River (Sweden) based upon the viscosity models shown in (a).

produce the complex but almost monotonic variation of polar wander speed as a function of the upper mantle–lower mantle viscosity contrast first described in Peltier (1988) (see his fig. 3) although they appear to have been unaware of this work. An earlier analysis of the dependence of polar wander speed on lower mantle viscosity with the upper mantle viscosity held fixed to 10^{21} Pa s was presented by Yuen et al. (1986) but their result was characterized by a very much higher degree of non-

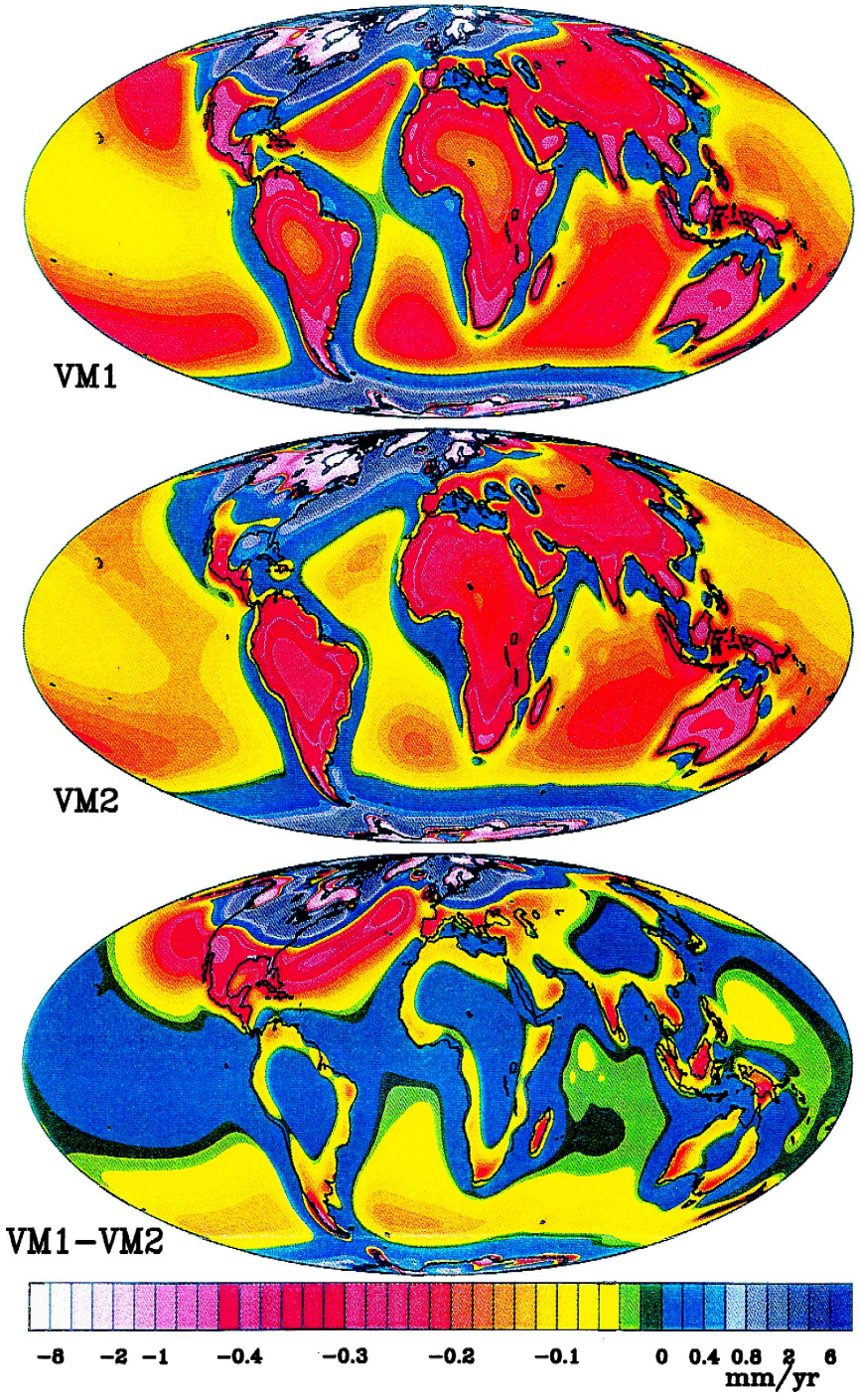

Fig. 4. The present-day rate of relative sea level rise predicted by the global theory of glacial isostatic adjustment using (a) the VM1 viscosity model and (b) the VM2 viscosity model. Both calculations of this signal employ the ICE-4G deglaciation history of Peltier (1994, 1996a,b). The difference between the VM1 and VM2 based signals is shown on (c).

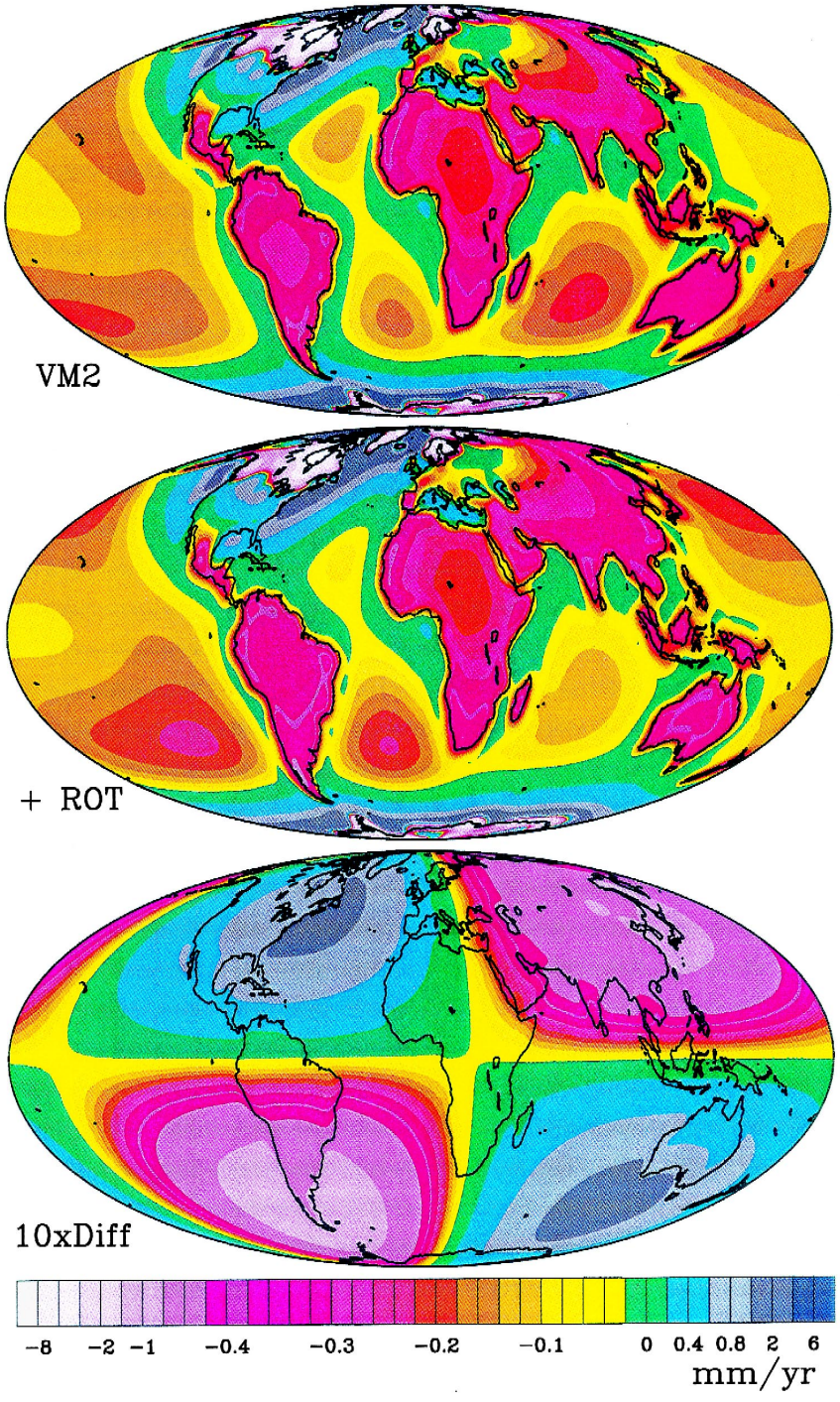
Effect of Rotation on
Rate of change of Sealevel
VM2
+ ROT
10xDiff
−8 −2 −1 −0.4 −0.3 −0.2 −0.1 0 0.4 0.8 2 6
mm/yr

monotonicity of the dependence than that obtained with more realistic models. Detailed analyses of two-layer VM1-type models of the mantle viscosity stratification and for a variety of models of the history of surface loading have recently been presented in Peltier (1997) and no useful purpose will be served by reviewing these analyses herein. One point that is worth noting, however, is the significant difference in the results obtained when the Earth is treated as incompressible, as in Vermeersen and Sabadini (1996) rather than as compressible as in Milne and Mitrovica (1996) and Peltier (1997). Inspection of the results shown in Fig. 5 demonstrates that the magnitude of the influence of rotational feedback upon the present-day rate of global sea level rise is nevertheless very small. At most, at the four distinct extrema which characterize the degree two and order one pattern of the rotational effect, the effect is less than 0.2 mm yr^{-1}.

That this very modest influence of rotational feedback on the present-day rate of relative sea level rise extends to the full history of postglacial relative sea level change is demonstrated in Fig. 6. On this figure show complete relative sea level histories for six sites on the earth's surface, two of which (the Island of Barbados and the Huon Peninsula of Papua, New Guinea) are sites at which long records of relative sea level change are available based upon U/Th dated coral sequences. Also shown are results for four sites that are each located close to one of the 'bulls-eyes' of the degree two and order one pattern that characterizes the rotational effect. (It should be clear that the explanation of the dominance of this pattern lies in the fact that the influence of polar motion on the centrifugal forcing dominates that due to the change of the rate of rotation). On this figure and at each of the six sites I show both the relative sea level history predicted with and without rotational feedback. The difference between the latter and the former is also shown on an expanded scale in the inset to each figure. These results demonstrate very clearly that the impact of rotational feedback on relative sea level history is extremely small, in fact between one and two orders of magnitude less than recently suggested on qualitative grounds by Bills and James (1996). Of special interest from the perspective of this paper is the result shown for Clinton, CT on the east coast of the continental United States. This site lies very close to one of the extrema in the rotational impact pattern and inspection of the results at this site demonstrates that the rotational feedback slightly diminishes the rate of relative sea level rise along this coast by a maximum amount near 0.2 mm yr^{-1}. As we will see, an influence of this magnitude is not significant given the noise level that is characteristic of the observations in this region and the fact that the strength of the signal is near 2 mm yr^{-1}.

3. US east coast relative sea level histories

Fig. 7 shows location maps for sites along the US east coast from which both tide gauge estimates of secular sea level trends are available based upon records that are at least 60 years long (Douglas, 1991) and for sites from which radiocarbon dated rsl histories have also been constructed. The latter sites are those in the archive of Tushingham and Peltier (1992). Although a brief intercomparison of these data has been presented previously by Peltier (1996a), the result obtained is sufficiently important that several variants of the original analysis will be reported herein in order to confirm the stability of the original inference. The main variation that we will perform involves comparing the results obtained using the compilation of the ^{14}C data in Tushingham and Peltier (1992) with those obtained using data from the same sites but compiled differently. In Tushingham and Peltier (1992) the ^{14}C dated rsl curves were represented by discretely sampling the envelope of the region within which the totality of the rsl data points were contained at each site. Here we will compare the final result obtained in the tide gauge–^{14}C comparison using either these 'Envelope' data or

Fig. 5. Predictions of the present-day rate of sea level rise based upon the ICE-4G (VM2) model. Results are shown both excluding (top plate) and including (middle plate) the influence of rotational feedback. The bottom plate shows the difference between these two predictions which is simply the rotational feedback effect itself.

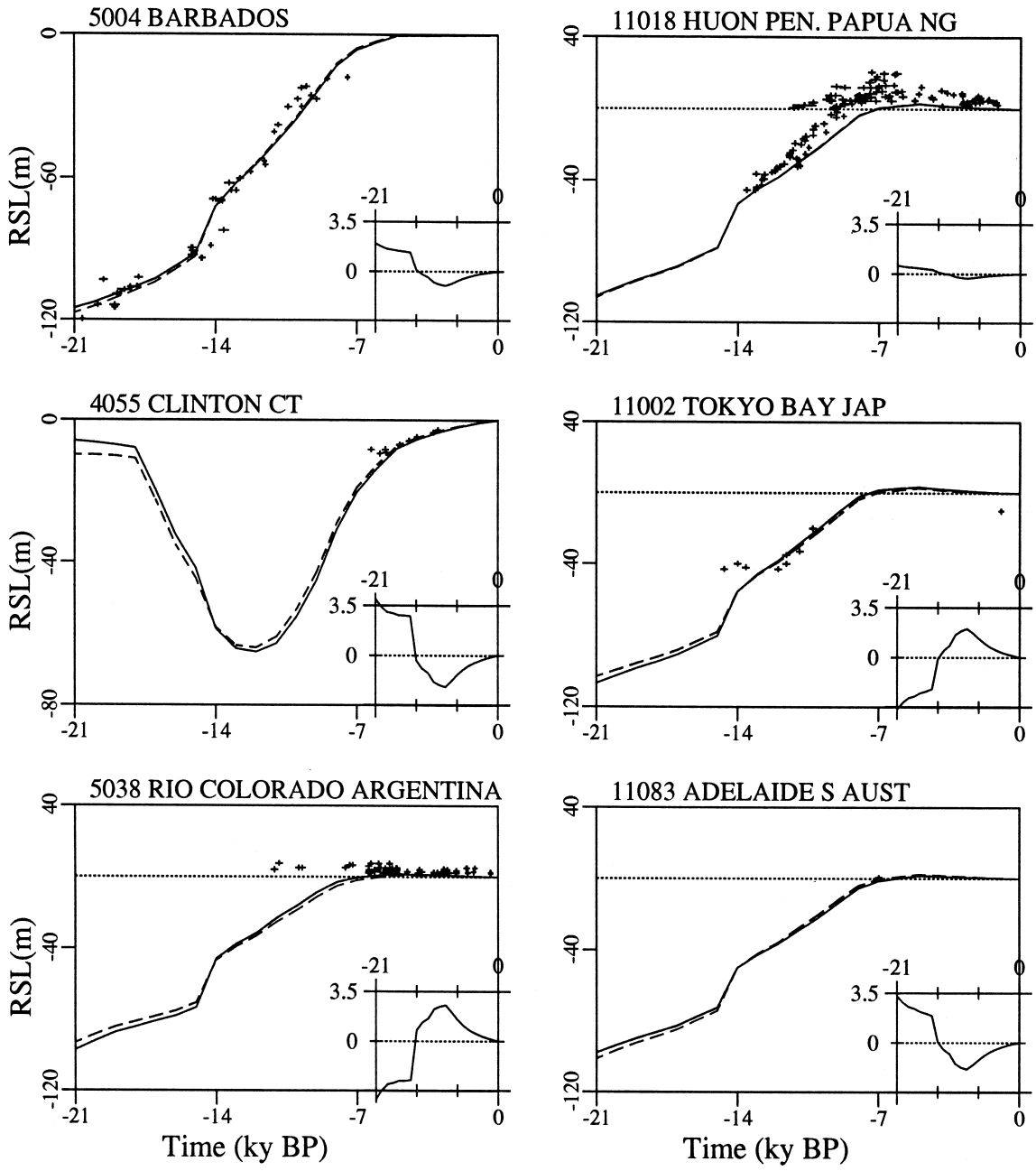

Fig. 6. Relative sea level histories at six sites compared with predictions of the ICE-4G (VM2) model based upon analyses that both exclude (solid lines) and include (dashed lines) the influence of rotational feedback. The first two sites (Barbados and the Huon Peninsula) are locations from which long coral based records of relative sea level history are available. The remaining four sites are each located near one of the locations at which the rotational effect achieves a local extremum.

the re-compiled 'Raw' data. In Fig. 8a–d, I present these two alternate forms of the ^{14}C data for each of the 16 sites on the US east coast shown on Fig. 7. On each of the data sets shown for individual sites

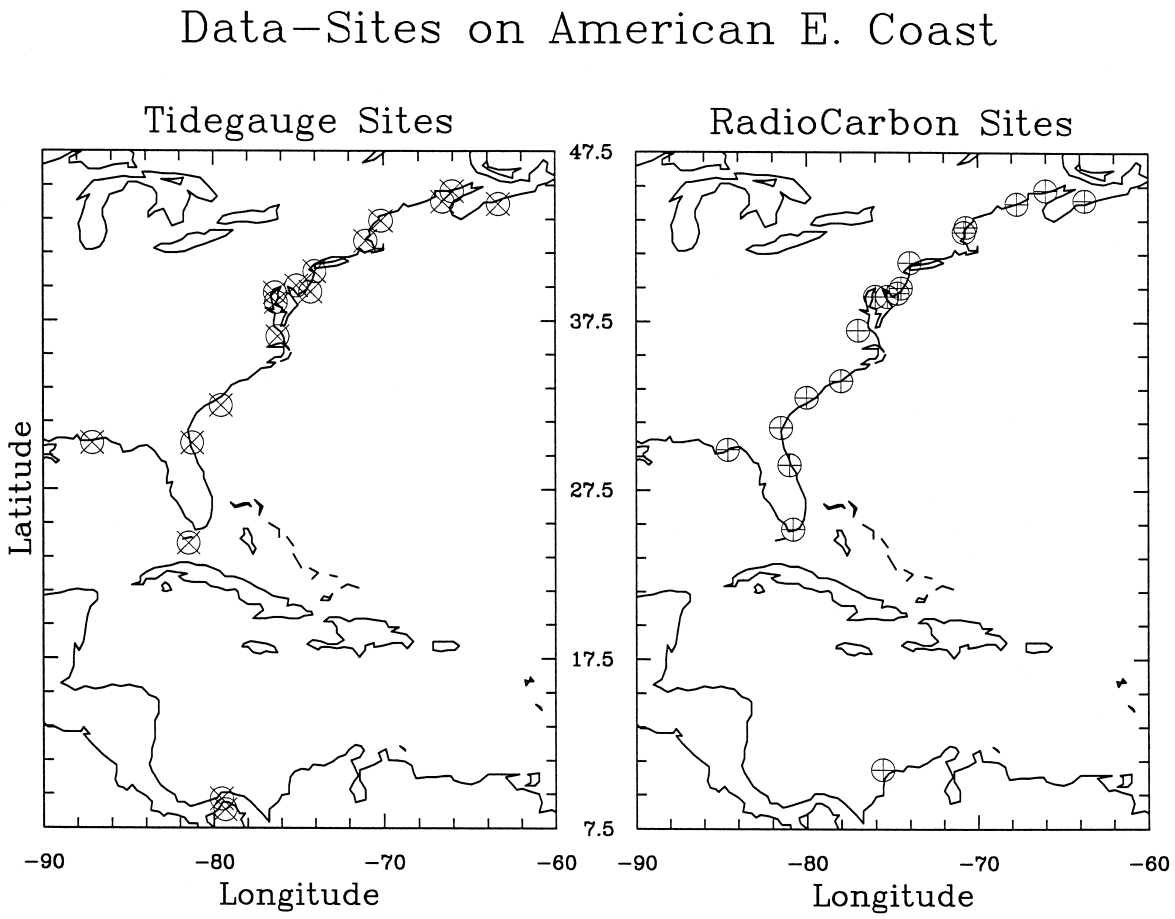

Fig. 7. Location of sites along the US east coast from which tide gauge records are available that are sufficiently long to allow accurate estimation of the secular trend of sea level. These locations are as discussed in Douglas (1991, 1995). Also shown are the locations of the sites in the archive of Tushingham and Peltier (1992) from which radiocarbon dated relative sea level histories are available which may also be employed to determine the secular variation of sea level on the longer (millennium) timescale over which sea level change is dominated by the glacial isostatic adjustment process.

on Fig. 8, the solid lines are best, in a least-squares-sense, exponential fits to the relative sea level data. For each site location and each data set type, two numbers are shown for the present-day rate of relative sea level rise estimated from the data. The first of these is based upon direct differentiation of the best fit exponential whereas the second (in brackets) is based upon a subjective estimate determined on the basis of a smooth curve fit to the data neglecting outlying points entirely. Table 1 lists a series of four to seven different estimates of the ^{14}C determined present-day rate of rsl rise for each of the 16 sites along the US east coast shown on Fig. 7b.

The present-day rate of relative sea level rise as a function of position along the US east coast determined at the tide gauge site locations shown on Fig. 3a is shown for both the tide gauge data and the ^{14}C data on Fig. 9. On each of the six frames of this figure are shown the secular rates of present-day sea level rise based upon the tide gauge analyses of Douglas (1991) and based upon either one or the other of the six basic analysis procedures to which the ^{14}C data have been subjected as discussed above. Also shown for each of these variants on the analysis procedure is the difference between the tide gauge rates (dotted lines) and the ^{14}C rates (solid lines), this

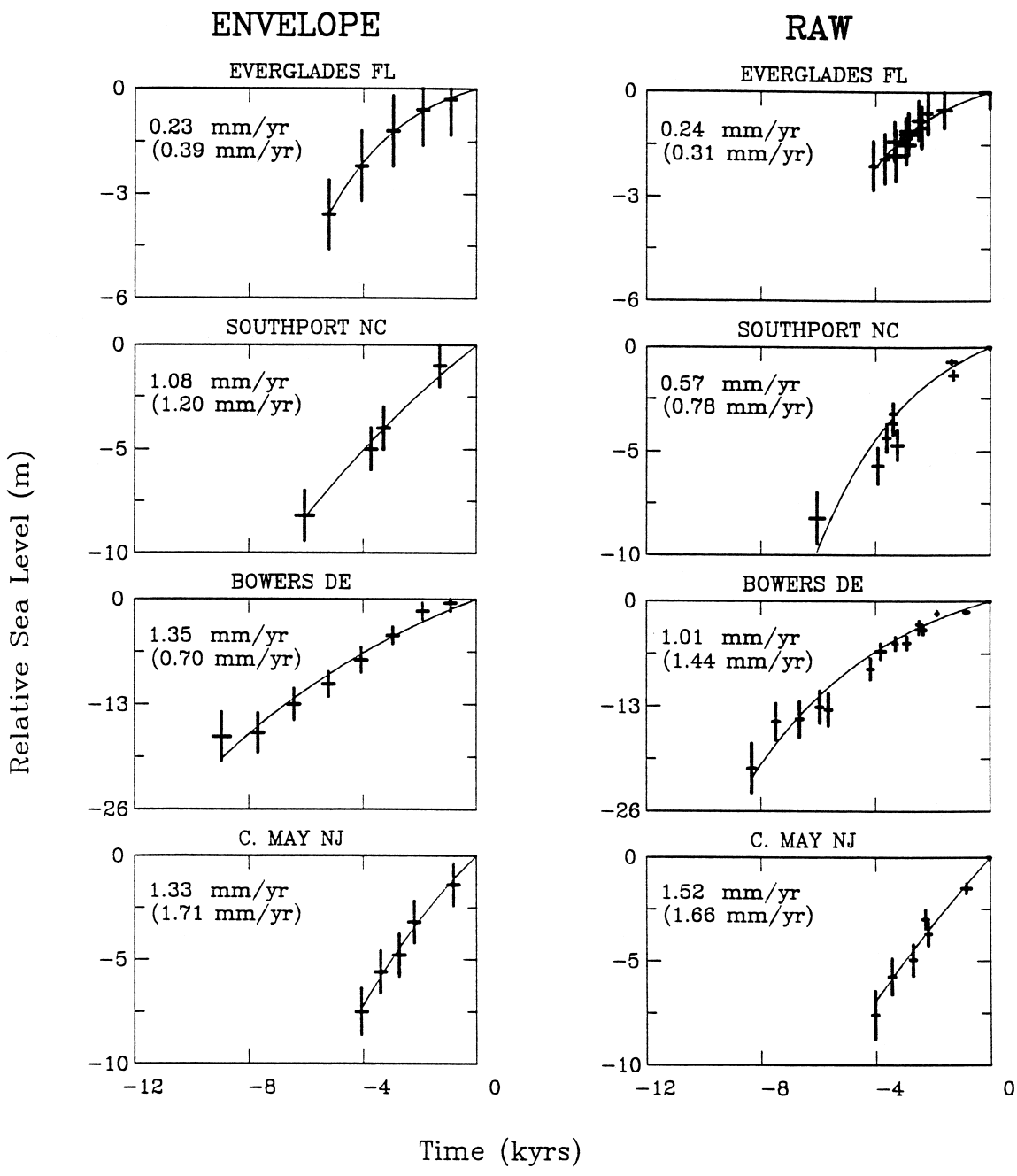

Fig. 8. Radiocarbon data sets from the 16 locations along the US east coast which are employed to 'decontaminate' the tide gauge records of the influence of glacial isostatic adjustment. For each site, two versions of the 'data' are presented, one consisting of the sampled 'envelope' as this was compiled by Tushingham and Peltier (1992) and the other consisting of the 'raw' age–height pairs of data points as listed in the original publications from which the Tushingham and Peltier compilation was assembled. On each frame and for each data type is shown a best fit exponential curve and also two estimates of the present-day rate of rsl rise (in mm yr^{-1}), one based upon direct differentiation of the smooth exponential fit and another based upon a subjective estimate (see Table 1).

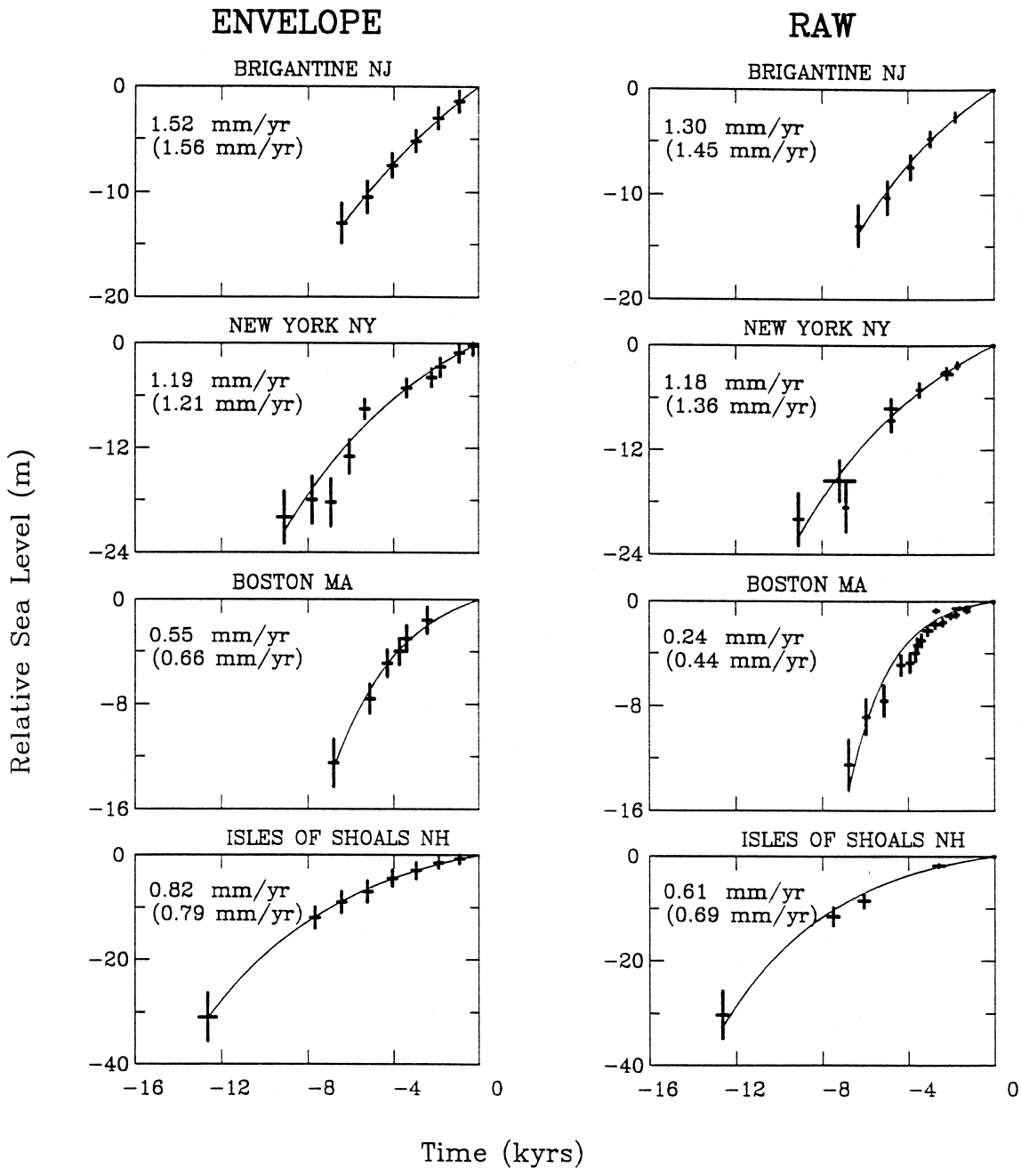

Fig. 8 (continued).

difference being denoted by the dashed line in each case. Also displayed is the latitudinal average of the difference signal along with a standard deviation. Plates (a)–(c) of Fig. 9 are respectively based upon treating the 'raw' ^{14}C data as exponential (a), subjectively analysed (b) or by best fitting, in a least-

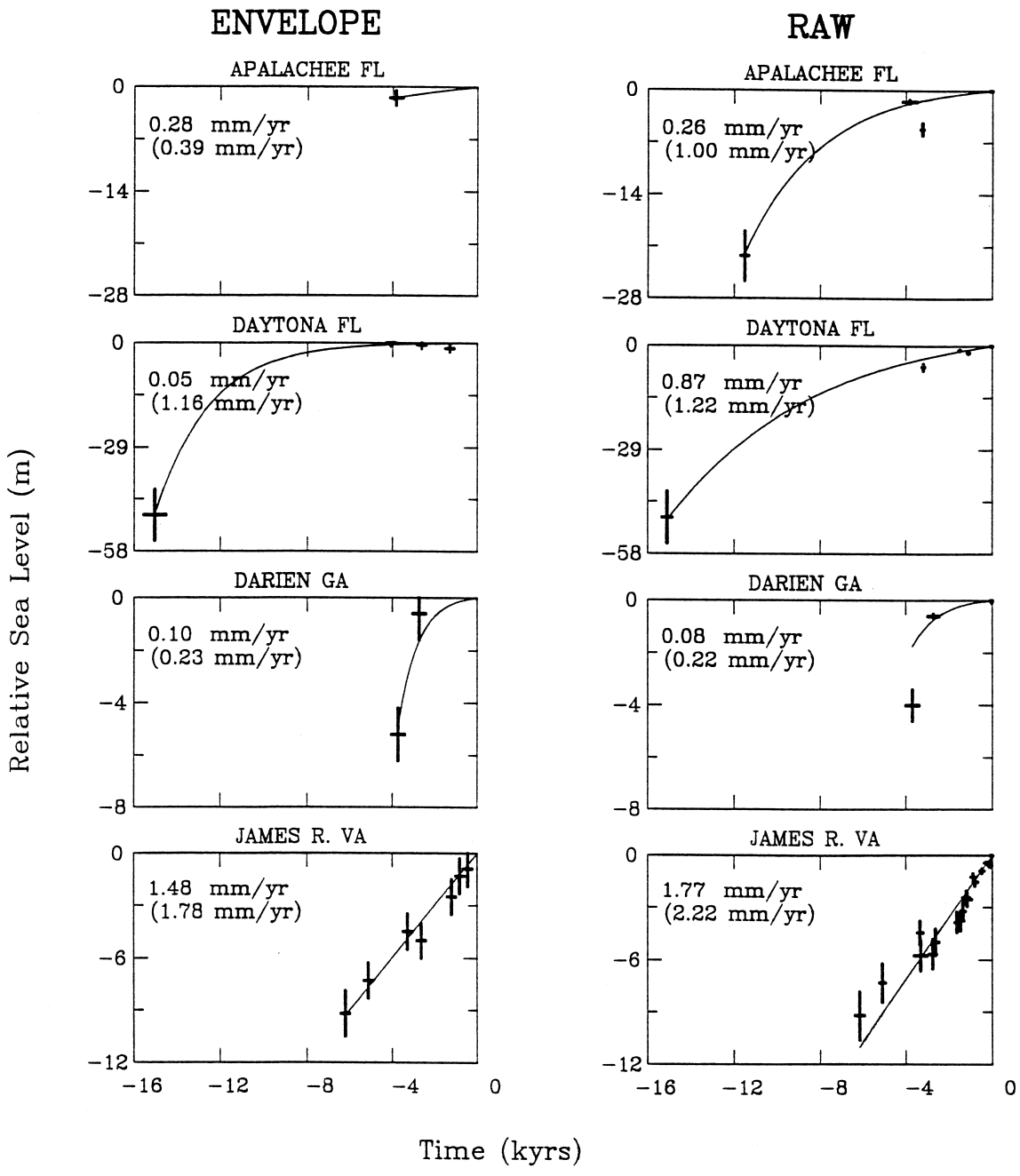

Fig. 8 (continued).

squares-sense, a straight line to the youngest data points (c). Likewise the results shown on plates (d)–(f) were obtained by applying the same three analysis procedures to the 'envelope' data in the original Tushingham and Peltier (1992) archive. The values obtained for the present-day rate of relative

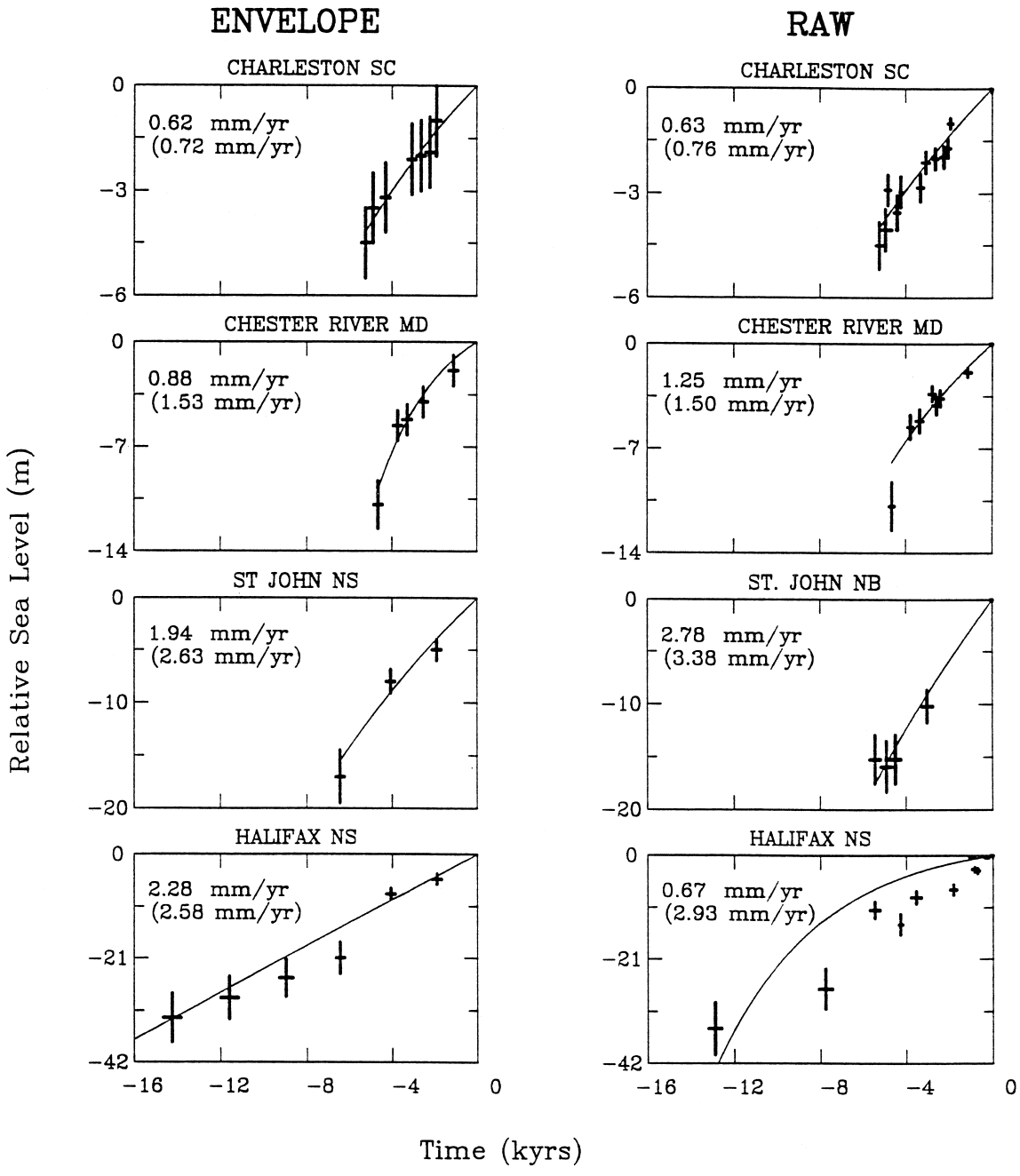

Fig. 8 (continued).

sea level rise at the tide gauge locations based upon these different procedures for analysing the ^{14}C data are listed in Table 1.

Inspection of the results shown for the three different analysis procedures, applied to both the 'envelope' and 'raw' ^{14}C data, demonstrates that the

Table 1
Rate of sea level rise at ^{14}C locations (in mm yr^{-1}) used to compare with tide gauge data

Site number (Tushingham–Peltier 1992 archive)	Location	Exponential fit		Subjective determinations		Least squares straight line fits		
		Raw	Envelope	Slope to 1st pt	Hand drawn smooth curve	1 kyr	2 kyr	3 kyr
320	St. John, NB	2.78	1.94	3.38	3.38	–	–	–
321	Addison							
316	Halifax	0.67	2.28	1.48	2.93	2.27	3.14	3.14
322	Is of Shoals	0.61	0.82	0.69	0.69	–	–	0.69
323	Boston	0.24	0.55	0.33	0.44	–	0.45	0.50
328	New York	1.18	1.19	1.32	1.36	–	1.32	1.40
335	Bowers	1.01	1.35	1.59	1.44	1.59	0.95	1.42
333	Brigantine	1.30	1.52	1.45	1.45	–	1.45	1.55
334	Cape May	1.52	1.33	1.78	1.66	1.78	1.78	1.65
336	Chester R	1.25	0.88	1.67	1.50	–	1.67	1.43
338	James R	1.77	1.48	5.56	2.22	1.68	2.22	2.08
342	Charleston	0.63	0.62	0.51	0.76	–	0.51	0.75
344	Darien	0.08	0.10	0.22	0.22	–	–	0.22
345	Daytona	0.87	0.05	1.71	1.22	–	1.07	1.07
347	Apalachee	0.26	0.28	1.60	1.00	–	−0.23	−0.23
346	Everglades	0.24	0.23	0.31	0.31	–	0.31	0.40

The pairings of tide gauge and ^{14}C stations employed is the same as that discussed in detail in Peltier and Jiang (1997).

discrepancy between the latitudinal average of the difference between the tide gauge derived rates and the ^{14}C derived rates is extremely modest. The result for each procedure is extremely close to 2 mm yr^{-1} with a standard deviation near 0.7 mm yr^{-1}. This stable estimate should be compared with the rate originally inferred by Tushingham and Peltier (1992) based upon a global EOF based analysis which yielded, for the glacial isostatic adjustment corrected rate of relative sea level rise, a value of 2.4 ± 0.9 mm yr^{-1}. Clearly the totality of the data from sites along the US east coast accurately constrain the local value of the rate of relative sea level rise that is in excess of the rate expected due to the influence of ongoing glacial isostatic adjustment in this region where sea level is currently rising, in part, as a consequence of the collapse of the pro-glacial forebulge.

Given the stability of the residual rate of rsl rise along the US east coast it would appear that the ^{14}C data from this region vary as a function of latitude in a way that must be explicable in terms of the single dominant process of glacial isostatic adjustment. It is therefore important that any model that is employed to represent the global characteristics of this process should fit the US east coast data as accurately as possible. It has in fact been established in Peltier (1996a) that, whereas viscosity model VM1 drastically misfits US east coast ^{14}C data, viscosity model VM2 essentially eliminates the majority of these misfits. In Section 4 we will present an important and novel example of a global sea level prediction from the ICE-4G and VM2 based model of global glacial isostatic adjustment.

Prior to discussing this example, however, it is useful at this point to return to a discussion of the suite of additional viscosity models shown in part (b) of Fig. 1. On this figure show the impact upon the formally inferred viscosity model of correcting one of the data used in the formal viscosity inversion for the influence of the global rate of sea level rise discussed in this section, based upon the assumption that a significant fraction of this signal requires an explanation in terms of the present-day melting of land ice. If the location at which land ice is melting is either Greenland or Antarctica then the magnitude of the correction that must be applied to the observed nontidal component of the acceleration of axial rotation (or equivalently $\dot{J}_2$) is essentially the same for a given contribution to the global sea level rise signal (Peltier, 1988; Mitrovica and Peltier, 1991). Since the rotational data are the only observations that significantly constrain the viscosity of the deepest mantle, it should not be surprising that it is in this region that the formally inferred viscosity profile is altered when the rotational observables are corrected to include the influence of the ongoing global rise of sea level that some believe may have an origin in ongoing global climate change. In part (b) of Fig. 1, I show the sequence of modifications to VM2 that are required if the observed $\dot{J}_2$ is modified by subtracting the contribution due to present-day global sea level rise at rates from 0.5 to 1.5 mm yr^{-1}, it being normally expected that the maximum contribution to the global signal that could be associated with the steric effect of the thermal expansion of sea water is near 0.5 mm yr^{-1}. Based upon inspection of the modifications to VM2 that follow from allowing for the contribution to $\dot{J}_2$ due to the melting of land ice, it is clear that this leads to a substantial increase in the viscosity inferred for the deepest part of the lower mantle. As discussed in Peltier (1996b) it is just an increase of this sort that seems to be required to reconcile the aspherical geoid anomalies that are supported by the mantle convection process although the meaning of this remains unclear (see Peltier, 1998, for further discussion of this point).

Since these results for viscosity are based solely upon adjustment of the $\dot{J}_2$ datum for the influence of polar ice-sheet melting, it is clearly important to

Fig. 9. (overleaf) Comparisons of ^{14}C determined and tide gauge determined rates of sea level rise from sites that span the entire north–south extent of the US east coast. On each of the frames (a)–(f) the dotted curve is based upon the tide gauge derived rates, the solid curve is based upon the radiocarbon derived rates and the dashed curve is the difference, the latitudinal average value of which, along with the standard deviation, is also given. In plates (a)–(f) the data employed are the 'raw' data whereas in Plates (d)–(f) the 'envelope' data were employed. In (a)–(c) the ^{14}C rates were determined using the exponential fit, the subjective fit and the least squares fit, respectively (see Table 1). The same sequence of three procedures were employed to produce the data sets shown in (d)–(f).

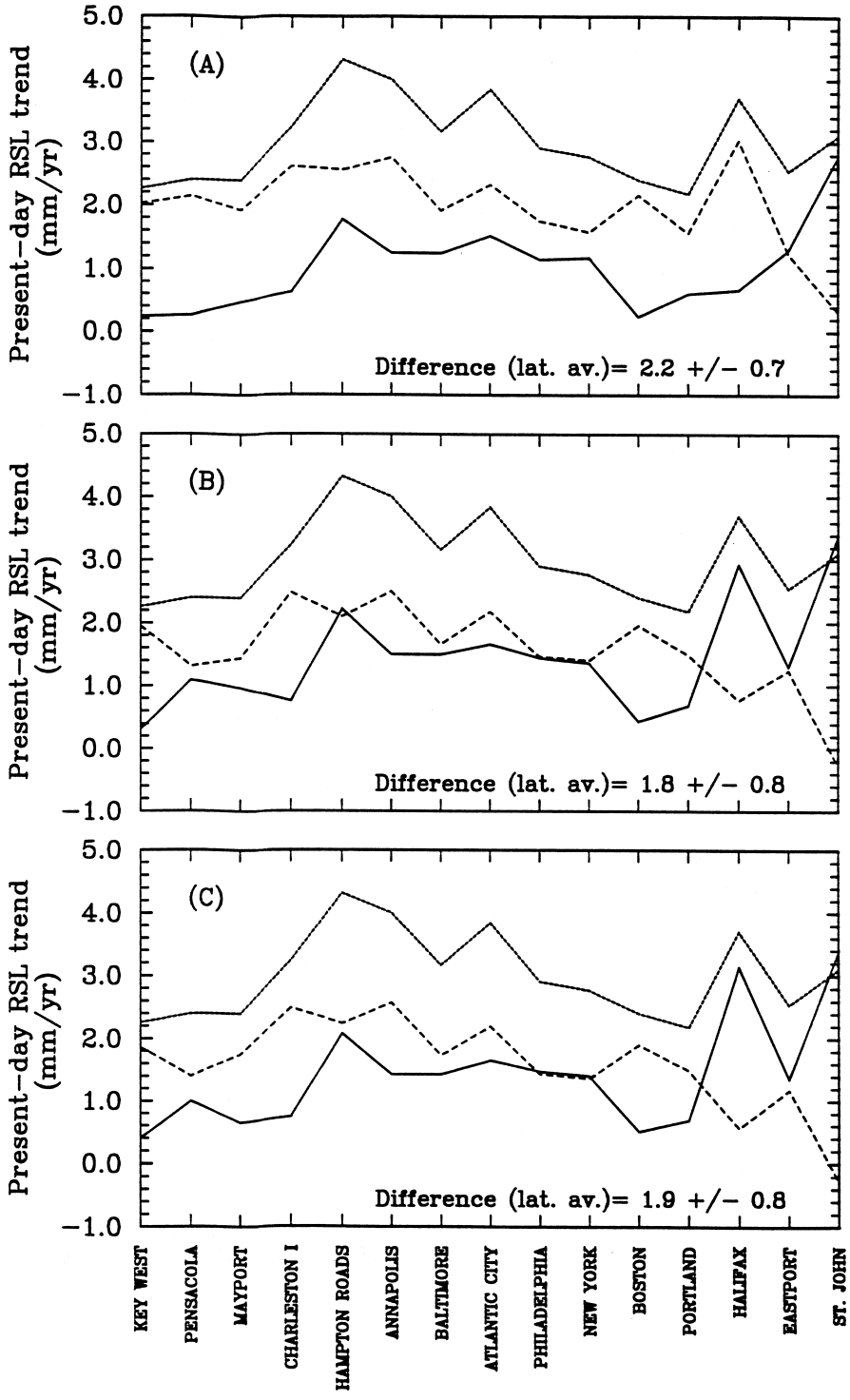
(A)
Difference (lat. av.)= 2.2 +/− 0.7
(B)
Difference (lat. av.)= 1.8 +/− 0.8
(C)
Difference (lat. av.)= 1.9 +/− 0.8
Present−day RSL trend (mm/yr)
5.0
4.0
3.0
2.0
1.0
0.0
−1.0
KEY WEST
PENSACOLA
MAYPORT
CHARLESTON I
HAMPTON ROADS
ANNAPOLIS
BALTIMORE
ATLANTIC CITY
PHILADELPHIA
NEW YORK
BOSTON
PORTLAND
HALIFAX
EASTPORT
ST. JOHN

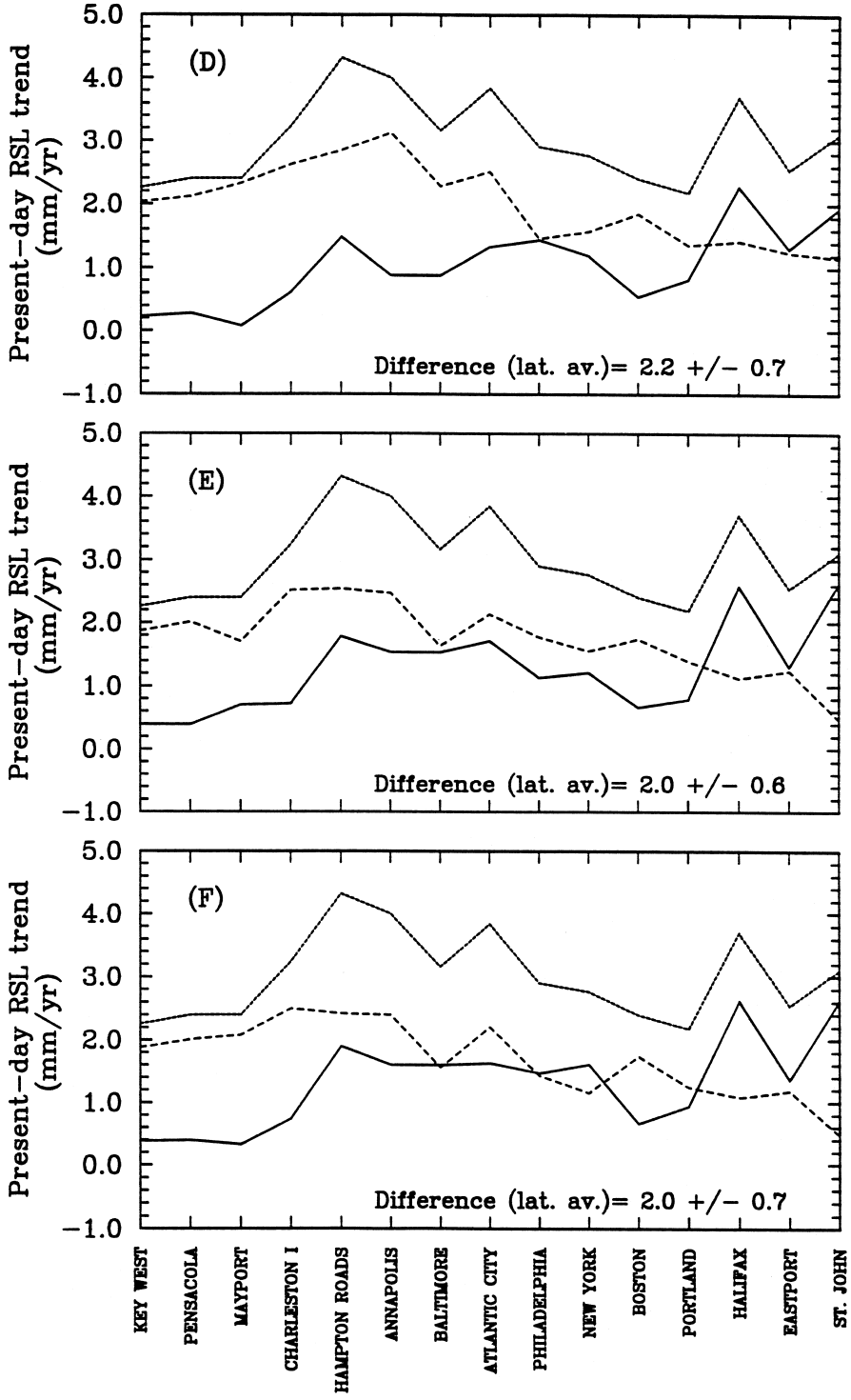

Fig. 9 (continued).

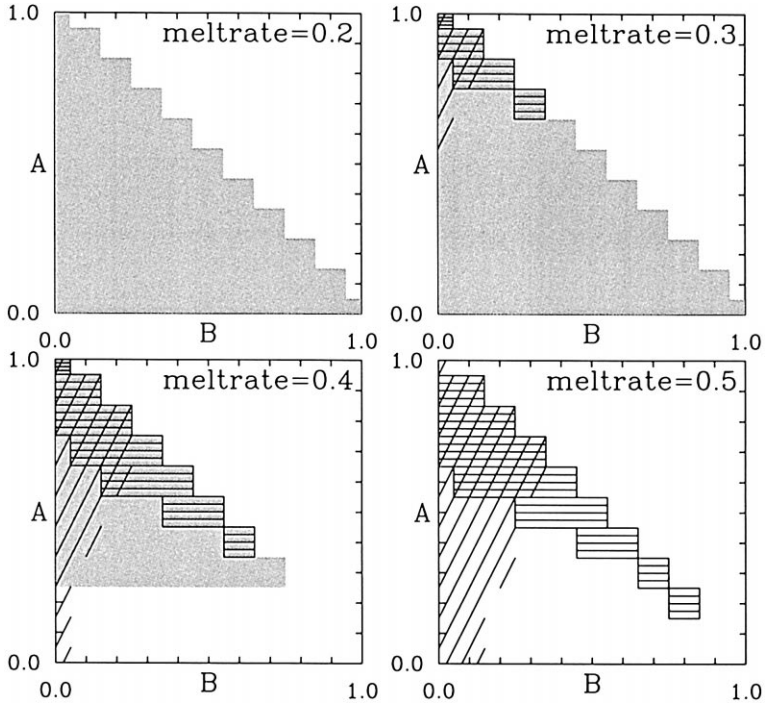

Fig. 10. Rotational response results for the three observables consisting of $\dot{J}_2$, polar wander speed and polar wander direction. For four different choices of the total 'Rate' of global sea level rise this figure illustrates the regions in the A–B plane defined by Eq. (15) in which it is possible to fit each of the rotational observables within the rather generous error bounds listed in Eqs. (14a), (14b) and (14c). Agreement with the observed $\dot{J}_2$ is achieved within the region denoted by the grey scale, for polar wander speed by the diagonally hatched region and for polar wander direction by the horizontally hatched region. The parameters A and B represent the fractions of 'Rate' that are contributed from Greenland and West Antarctica whereas that from East Greenland is simply $1-A-B$. For each calculation I have assumed that the small ice sheets and glaciers contribution of Meier (1984) has a net strength corresponding to a global rate of relative sea level rise of 0.8 mm yr^{-1} (the upper bound of Meier's estimate). In each case the contribution due to the GIA process is computed using the ICE-4G (VM3) model.

enquire as to whether and under what conditions the model so derived is able to simultaneously reconcile the other rotational constraints. In order to investigate this important issue we may proceed by assuming that the VM3 viscosity model is 'correct', this being the model inferred by assuming that the $\dot{J}_2$ datum is biased by the ongoing melting of polar ice such as to cause global sea level to rise at the rate of 1.5 mm yr^{-1}. This rate is the maximum rate that would usually be considered plausible. We then focus upon the three rotational observables, respectively $\dot{J}_2$ and polar wander speed and direction (see

Fig. 11. Part (a) shows the present-day rate of sea level rise relative to the surface of the solid earth whereas part (b) shows the present-day rate of radial displacement. Both results are obtained on the basis of the global theory described in Section 2 of this paper and do not include the influence of the second-order effect on sea level change due to feedback upon sea level associated with the changing rotation. Part (c) shows the sum of the fields in (a) and (b) and this represents the present-day rate of change of sea level relative to the centre of mass of the earth. This field is also shown over the continents simply because the geoid also has a precise definition over the continents even though its height cannot be observed altimetrically. Over the range of latitudes observed by the TOPEX/POSEIDON system, from approximately $-63°$ latitude to $+63°$ latitude, this signal is clearly negative and averages to a value near -0.4 mm yr^{-1}.

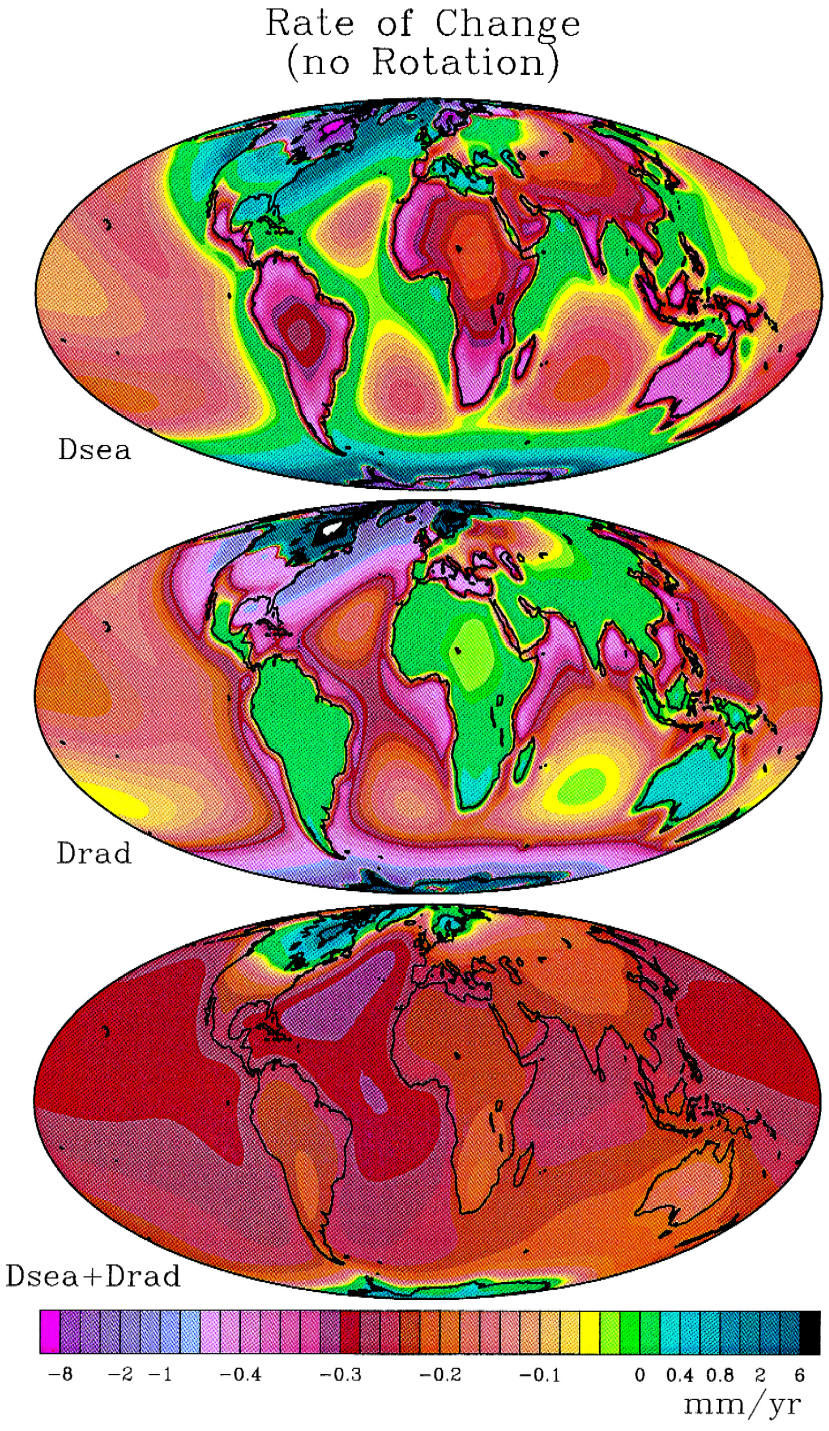
Rate of Change
(no Rotation)
Dsea
Drad
Dsea+Drad
−8 −2 −1 −0.4 −0.3 −0.2 −0.1 0 0.4 0.8 2 6
mm/yr

Peltier and Jiang, 1996b for a full discussion of these data). Generous bounds upon these three observations are as follows:

$$-2.0\times10^{-11}\ \mathrm{yr}^{-1} \le \dot{J}_2 \le 4.0\times10^{-11}\ \mathrm{yr}^{-1} \quad (14a)$$

$$0.75^\circ\ \text{million yr}^{-1} \le \text{PW speed} \le 1.1^\circ\ \text{million yr}^{-1} \quad (14b)$$

$$70^\circ\ \text{east lang.} \le \text{PW direction} \le 8.2^\circ\ \text{east long.} \quad (14c)$$

We then proceed to calculate the total values of each of the rotational observables (Response) by assuming them to consist of the superposition of the following distinct influences:

$$\begin{aligned}\text{Response} = {} & \text{ICE} - 4\text{G(VM3)} + \text{Meier} \\ & + \text{Rate}(A\cdot\text{Greenland} + B \\ & \cdot\text{West Antarctica} + (1-A-B) \\ & \cdot\text{East Antarctica})\end{aligned} \quad (15)$$

The contribution to the response labelled 'Meier' is that due to the melting of small ice sheets and glaciers described by Meier (1984) as first computed in Peltier (1988). Since this contribution is known and since the full ice-age effect is also known on the basis of the ICE-4G (VM3) calculation we may therefore enquire as to the values of A, B and Rate for which it is possible to fit the observations within the above described limits. In the above expression the parameter 'Rate' is the total rate of rsl rise that is assumed to be delivered by melting of the present-day Greenland, West Antarctic and East Antarctic ice-sheets. The parameters A, B and $1-A-B$ are the fractions of the total 'Rate' that are contributed by the melting of polar ice at these three respective locations.

Fig. 10 shows a sequence of results based upon this calculation, in the A–B plane for various values of 'Rate'. In this plane the regions within which it is possible to fit the observational constraints are shown as grey scale (for $\dot{J}_2$), diagonally hatched (for PW speed) and horizontally hatched (for polar wander direction). Clearly, only the region of intersection of these three spaces defines the range of acceptable solutions. Inspection of these results demonstrates that acceptable solutions are characterized by $A \simeq 1$, implying that no solutions exist that are characterized by significant melting occurring on either west or east Antarctica. Furthermore, the largest values of 'Rate' for which solutions exist for this choice of viscosity profile are 0.4 mm yr^{-1} at largest. Since the rate of rsl rise associated with the melting of Meier's sources has been assumed to be 0.8 mm yr^{-1} (his upper bound) this means that at most 1.2 mm yr^{-1} of the observed rate near 2 mm yr^{-1} could be due to the present-day melting of land ice. If the rate at which global sea level is presently rising is in fact near 2 mm yr^{-1} this would imply that the steric effect of the thermal expansion of the oceans must be much larger than the 0.5 mm yr^{-1} that is conventionally assumed. Church et al. (1991) have in fact argued that the influence of thermal expansion could be the dominant influence currently active in the earth system. The analyses presented herein provide some support for this view.

4. The GIA contribution to satellite altimetric measurements of global sea level

Because of the sparse coverage of the Earth's surface by tide gauge installations and because of the importance of global sea level rise in the context of modern global change research, it has been understood for some time that long time series of satellite altimetric measurements of sea level would be required to provide a definitive estimate of this signal. Although it might be imagined that the magnitude of the GIA influence on sea level would be such that the average over the ocean basins of this contribution to global sea level rise would be insignificantly small, this is not necessarily the case as I will demonstrate in this section.

Since a laser altimeter mounted on board an artificial Earth satellite measures sea level as a function of distance from the centre of mass of the planet, the spatial distribution of this signal need not be, and in general will not be, anything like the signal shown previously on Figs. 4 and 5. In these figures the present-day rate of relative sea level rise due to the glacial isostatic adjustment process was shown relative to the surface of the solid earth because it is precisely relative to this surface that the

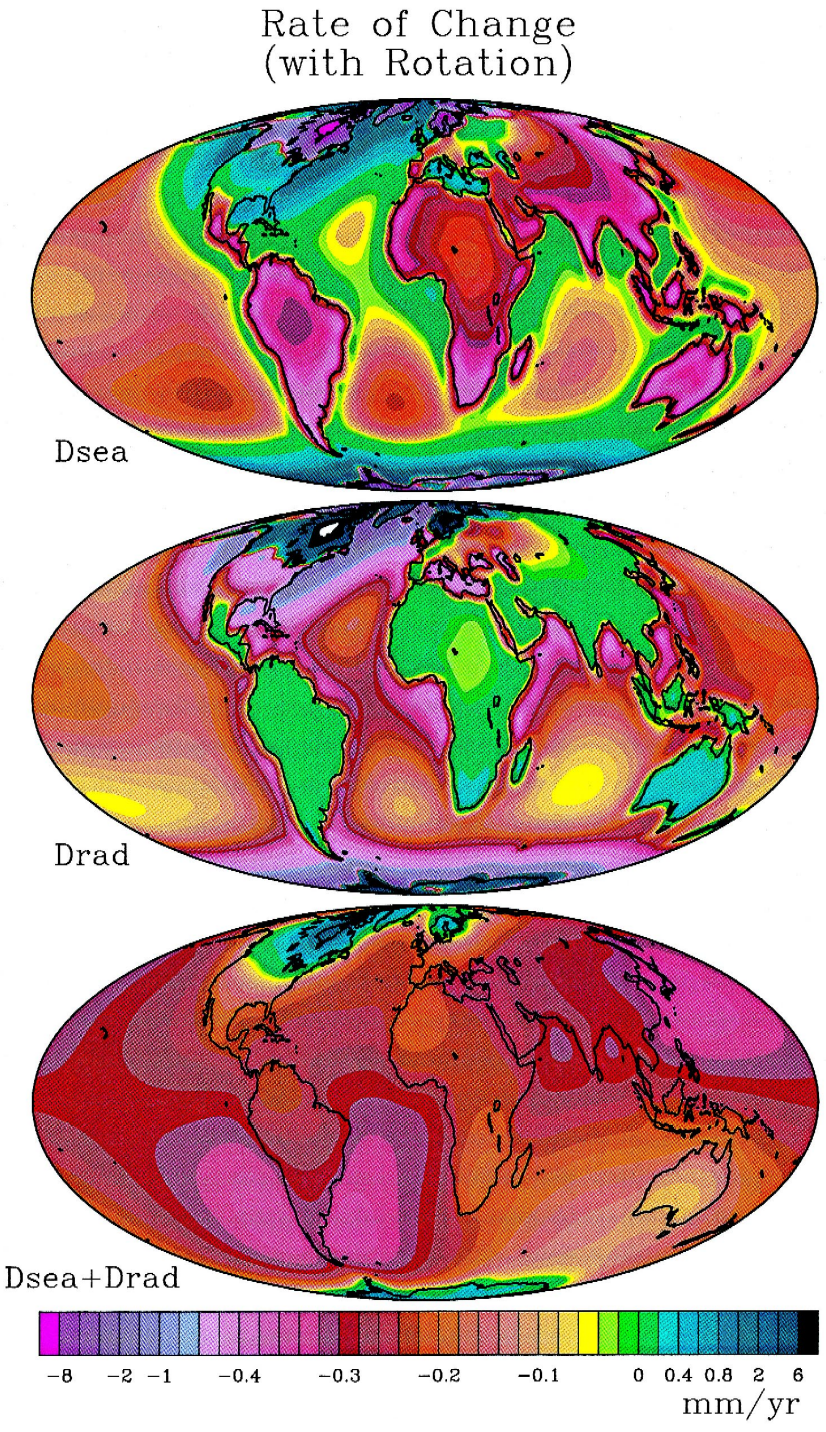

Fig. 12. Same as in Fig. 9 except that the influence of rotational feedback is included in the calculation based upon the ICE-4G (VM2) model. The upper plate is relative sea level, the middle plate is radial displacement and the lower plate shows the sum of these two fields and is therefore the rate of change of geoid height.

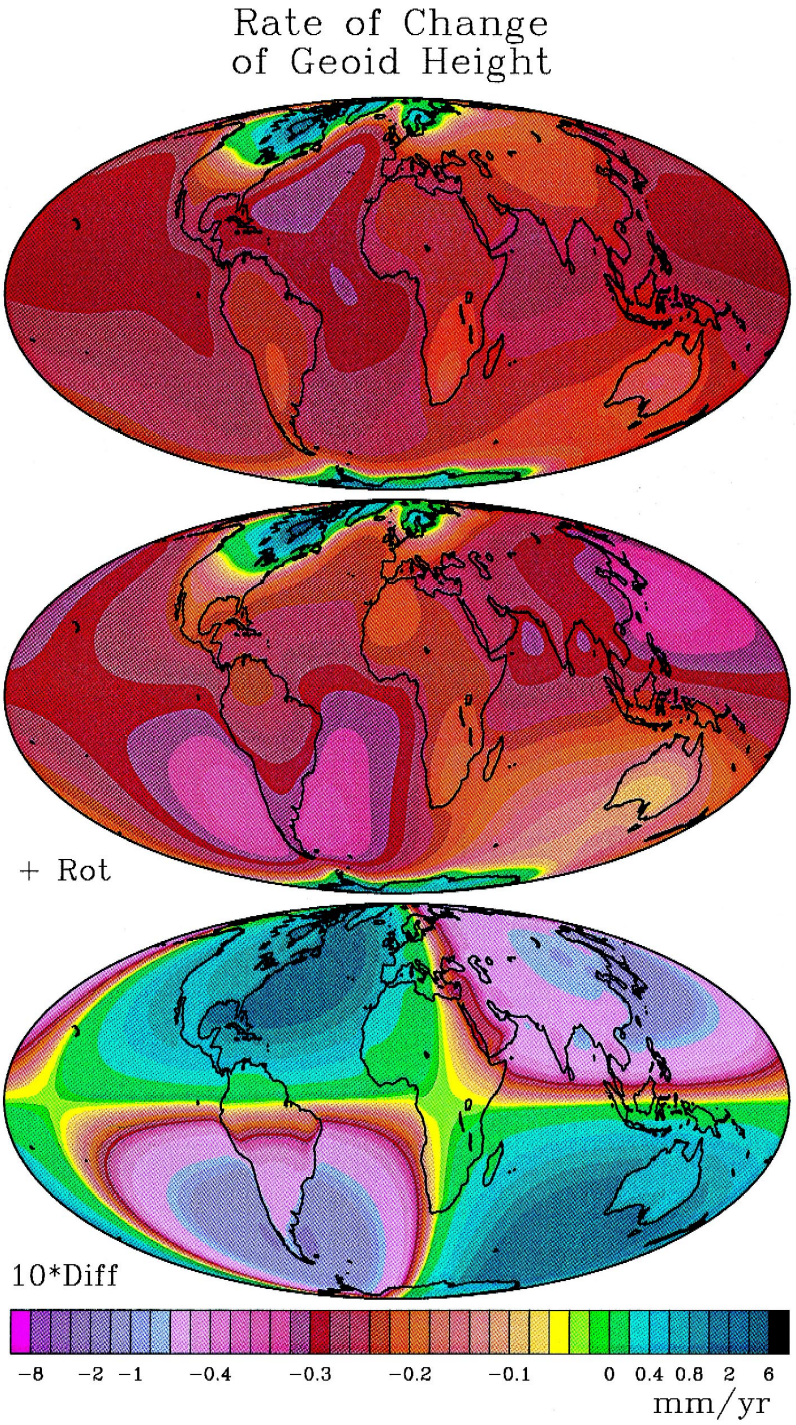

Fig. 13. Predicted present-day rates of change of geoid height for models that both include (middle) and exclude (upper) the influence of rotational feedback as well as the difference between them (lower plate).

^{14}C dated 'geological memory' of sea level is inscribed. The present-day rate of relative sea level rise due to GIA that would be observed by a satellite altimeter such as TOPEX, however, being a measurement relative to the centre-of-mass rather than relative to the solid surface, will clearly be the sum of the present-day rate of radial displacement of the Earth's surface relative to the centre of mass of the solid earth due to GIA and the present-day rate of rsl change relative to the solid surface. In Fig. 11, I therefore show for the first time the superposition of these two contributions to the GIA determined signal in sea level that would be observed altimetrically along with their sum. The first part of this figure shows the same rate of rsl change presented on Fig. 4 for the ICE-4G (VM2) model whereas the second shows the prediction for the present-day rate of radial displacement using the same model. The sum of these fields is shown in the bottom plate. Inspection of the figure shows that, over almost the entire portion of the surface covered by the current TOPEX-POSEIDON altimeter, the GIA signal is negative and reaches a maximum value near -0.4 mm yr^{-1}. When averaged over the ground track of the satellite, however, the signal strength is only -0.08 mm yr^{-1} (personal communication from Richard Rapp). This means that if the altimeter were to deliver a globally averaged rate of rsl rise of 1.9 mm yr^{-1} then this would imply the existence of a modern climate change related contribution to the global signal of 1.98 mm yr^{-1}. It is therefore very clear that GIA contamination of the signal in global sea level rise that a satellite altimeter would see is not extremely important though locally it could be highly significant.

Now the results for the rate of change of absolute sea level, or equivalently geoid height, shown in Fig. 11, were based upon an analysis performed by entirely neglecting the influence of rotational feedback. It is therefore interesting to enquire as to whether this influence might be more important on absolute sea level than on relative sea level. Fig. 12 therefore presents equivalent results to those shown in Fig. 11 for the ICE-4G (VM2) model but now including the rotational effect. Although the rate of change of geoid height shown on this figure is visibly distorted from the form shown on Fig. 11, there is no substantial change in amplitude as might have been anticipated on physical grounds. Fig. 13 shows the two predictions of the rate of charge of geoid height, with and without the influence of the changing rotation, as well as the difference between these two signals which will (of course) be observed to be identical to that shown on the last plate of Fig. 5. It therefore seems clear that the global rate of sea level rise that might be observable with TOPEX/POSEIDON and which will almost certainly be observable in the context of the NASA planned Gravity and Climate Experiment (GRACE) will not be significantly biased by the glacial isostatic adjustment effect.

5. Conclusions

In the previous sections of this paper I have attempted to summarize the current state-of-the-art in modelling the global process of glacial isostatic adjustment. Rather highly refined versions of this theory have now been developed which are capable of including second-order effects upon sea level associated both with the on-lap and off-lap of water from the continents and with the influence of the change in the planet's rotational state. As will be discussed elsewhere, the influence of rotation upon the TOPEX signal shown on Figs. 9 and 10 may, under certain circumstances of viscosity stratification, be nonnegligible. Its influence on the average of the global rate of sea level rise, however, is small, as is the average value of the GIA derived rate itself.

Although the main new result described in this paper is in fact this first prediction of the satellite altimetric signature of the GIA process, the new analyses of rsl data from the US east coast are also rather important. Our results in Section 3 demonstrate very clearly that the average rate of rsl rise along this coast, that is in excess of that explicable as a consequence of the GIA process of proglacial forebulge collapse, is near 2.0 mm yr^{-1}. This is fully compatible with the original result of Peltier and Tushingham (1989) that was obtained on the basis of an EOF analysis of the global tide gauge data set and with that of Douglas (1991, 1995, 1997) who employed the earlier ICE-3G based predictions of the influence of GIA to 'decontaminate' the tide gauge data.

References

Berger, A., 1978. Long term variations of daily insolation and Quaternary climate change. J. Atmos. Sci. 35 (12), 2362–2367.

Bills, B.G., James, T.S., 1996. Late Quaternary variations in relative sea level due to glacial cycle polar wander. Geophys. Res. Lett. 23, 3023–3026.

Church, J.A., Godfrey, J.S., Jackett, D.R., McDouglas, T.J., 1991. J. Clim. 4, 438–452.

Clark, J.A., Farrell, W.E., Peltier, W.R., 1978. Global changes in postglacial sea level: a numerical calculation. Quat. Res. 9, 265–287.

Dahlen, F.A., 1976. The passive influence of the oceans on the rotation of the Earth. Geophys. J. R. astr. Soc. 46, 363–406.

Douglas, B.C., 1991. Global sea level rise. J. Geophys. Res. 96 (4), 6981–6992.

Douglas, B.C., 1995. Global sea level change: determination and interpretation. Rev. Geophys. Suppl. 1425–1432, 1.

Douglas, B.C., 1997. Global sea level rise: a redetermination. Surveys Geophys. 18, 279–292.

Dziewonski, A.M., Anderson, D.L., 1981. Preliminary reference Earth model. Phys. Earth Planet. Int. 25, 295–356.

Farrell, W.E., Clark, J.A., 1976. On postglacial sea level. Geophys. J. R. Astron. Soc. 46, 647–667.

Forte, A.M., Mitrovica, J.X., 1996. New inferences of mantle viscosity from joint inversion of long wavelength mantle convection and postglacial rebound data. Geophys. Res. Lett. 23, 1147–1150.

Hager, B.H., Clayton, R.W., 1989. In: Peltier, W.R. (Ed.), Mantle Convection. Gordon and Breach, New York, pp. 657–763.

Hardy, L., 1976. Contribution a l'etude geomorphologique de la portion Quebecoise de la baie de James. PhD memoir, McGill University, 264 pp.

Hays, J.D., Imbrie, J., Shackleton, N.J., 1976. Variations in the earth's orbit: pacemaker of the ice ages. Science 194, 1121–1132.

Hillaire-Marcel, C., 1980. Multiple component postglacial emergence, Eastern Hudson Bay, Canada. In: Nils-Axel, M. (Ed.), Earth Rheology, Isostasy and Eustasy. Wiley, New York, pp. 215–230.

Houghton, J.T., et al. (Eds.), 1996. Climate Change 1995. Cambridge Univ. Press, Cambridge.

Lambeck, K., Johnston, P., Nakada, M., 1990. Holocene glacial rebound and sea level change in NW Europe. Geophys. J. Int. 103, 451–468.

McConnell, R.K., 1968. Viscosity of the mantle from relaxation time spectra of glacial isostatic adjustment. J. Geophys. Res. 73, 7089–7105.

Meier, M., 1984. Contribution of small glaciers to global sea level. Science 226, 1418–1421.

Milne, G.A., Mitrovica, J.X., 1996. Postglacial sea-level change on a rotating Earth: first results from a gravitationally self-consistent sea level equation. Geophys. J. Int. 126, F13–F20.

Mitrovica, J.X., Peltier, W.R., 1991. On postglacial geoid subsidence over the equatorial oceans. J. Geophys. Res. 96, 20053–20071.

Munk, W.H., MacDonald, G.F., 1960. The Rotation of the Earth. Cambridge Univ. Press, London.

Peltier, W.R., 1974. The impulse response of a Maxwell Earth. Rev. Geophys. Space Phys. 12, 649–669.

Peltier, W.R., 1976. Glacial isostatic adjustment: II. The inverse problem. Geophys. J. R. Astron. Soc. 46, 669–706.

Peltier, W.R., 1982. Dynamics of the Ice-age Earth. Adv. Geophys. 24, 1–146.

Peltier, W.R., 1985. The LAGEOS constraint on deep mantle viscosity: results from a new normal mode method for the inversion of viscoelastic relaxation spectra. J. Geophys. Res. 90, 9411–9421.

Peltier, W.R., 1988. Global sea level and earth rotation. Science 240, 895–901.

Peltier, W.R., 1994. Ice-age paleotopography. Science 265, 195–201.

Peltier, W.R., 1996a. Global sea level rise and glacial isostatic adjustment: an analysis of data from the east coast of North America. Geophys. Res. Lett. 23, 717–720.

Peltier, W.R., 1996b. Mantle viscosity and ice-age ice sheet topography. Science 274, 1359–1364.

Peltier, W.R., 1997. Correction to the paper 'Glacial isostatic adjustment and Earth rotation: refined constraints on the viscosity of the deepest mantle'. J. Geophys. Res. 102, 10101–10103.

Peltier, W.R., Andrews, J.T., 1976. Glacial isostatic adjustment I. The forward problem. I.R. Astron. Soc. 46, 605–646.

Peltier, W.R., Tushingham, A.M., 1989. Global sea level rise and the greenhouse effect: might they be connected?. Science 244, 806–810.

Peltier, W.R., Tushingham, A.M., 1991. Influence of glacial isostatic adjustment on tide gauge measurements of secular sea level change. J. Geophys. Res. 96, 6779–6796.

Peltier, W.R., Jiang, X., 1996a. Glacial isostatic adjustment and Earth rotation: refined constraints on the viscosity of the deepest mantle. J. Geophys. Res. 101, 3269–3290.

Peltier, W.R., Jiang, X., 1996b. Mantle viscosity from the simultaneous inversion of multiple data sets pertaining to postglacial rebound. Geophys. Res. Lett. 23, 503–506.

Peltier, W.R., Jiang, X., 1997. Mantle viscosity, glacial isostatic adjustment and the eustatic level of the sea. Geophys. Surveys 18, 239–277.

Peltier, W.R., Farrell, W.E., Clark, J.A., 1978. Glacial isostasy and relative sea level: a global finite element model. Tectonophysics 50, 81–110.

Peltier, W.R., 1998. Postglacial variations in the level of the sea: implications for climate dynamics and solid earth geophysics. Rev. Geophys. 36, 603–689.

Simons, M., Hager, B.H., 1997. Localization of the gravity field and the signature of glacial rebound. Nature 390, 500–504.

Stuiver, M., Reimer, P.J., 1993. Extended ^{14}C data base and revised Calib. 30 ^{14}C age calibration program. Radiocarbon 35, 215–230.

Tushingham, A.M., Peltier, W.R., 1992. Validation of the ICE-3G model of Würm–Wisconsin deglaciation using a global data base of relative sea level histories. J. Geophys. Res. 97, 3285–3304.

Vermeersen, L.L.A., Sabadini, R., 1996. Significance of the fundamental mantle relaxational mode in polar wander simulations. Geophys. J. Int. 127, F5–F9.

Walcott, R.E., 1980. Rheology models and observational data of glacio-isostatic rebound. In: Nils-Axel, M. (Ed.), Earth Rheology, Isostasy and Eustasy. Wiley, New York, pp. 3–10.

Wu, P., Peltier, W.R., 1983. Glacial isostatic adjustment and the free air gravity anomaly as a constraint on deep mantle viscosity. Geophy. J. R. Astron. Soc. 74, 377–449.

Wu, P., Peltier, W.R., 1984. Pleistocene deglaciation and the Earth's rotation: a new analysis. Geophys. J. R. Astron. Soc. 76, 202–242.

Yuen, D.A., Sabadini, R.C.A., Gasperini, P., Boschi, E., 1986. On transient rheology and glacial isostasy. J. Geophys. Res. 91, 11420–11438.